Chemie der Erde 75 (2015) 35–49

Contents lists available at ScienceDirect

Chemie der Erde

journal homepage: www.elsevier.de/chemer

Platinum-group elemental chemistry of the Baima and Taihe Fe–Ti oxide bearing gabbroic intrusions of the Emeishan large igneous province, SW China

J. Gregory Shellnutt[a,*], George S.-K. Ma[b,c], Liang Qi[d]

[a] Department of Earth Sciences, National Taiwan Normal University, 88 Section 4 Tingzhou Road, Taipei 11677, Taiwan
[b] Dragon Mining Consulting Limited, Unit 1901 AIA Financial Centre, 712 Prince Edward Road East, Kowloon, Hong Kong
[c] Institute of Earth Sciences, Academia Sinica, Taipei 11529, Taiwan
[d] State Key Lab of Ore Deposit Geochemistry, Institute of Geochemistry, Chinese Academy of Sciences, Guiyang 550002, China

ARTICLE INFO

Article history:
Received 19 September 2013
Accepted 20 June 2014
Editorial handling - A. Holzheid

Keywords:
Platinum group elements
Emeishan large igneous province
Oxide-bearing layered gabbroic intrusions
SW China
Permian

ABSTRACT

Nickel-, copper-, and platinum group element (PGE)-enriched sulphide mineralization in large igneous provinces has attracted numerous PGE studies. However, the distribution and behavior of PGEs as well as the history of sulphide saturation are less clear in oxide-dominated mineralization. Platinum group elements of oxide-bearing layered mafic intrusions from the Emeishan large igneous province are examined in this study. Samples collected from the Baima and Taihe oxide-bearing layered gabbroic intrusions reveal contrasting results. The samples from Baima gabbroic rocks have low total PGE abundances (ΣPGE < 4 ppb) whereas the Taihe gabbroic rocks, on average, have more than double the concentration but are variable ranging from ΣPGE < 2 ppb to ΣPGE ~300 ppb. The Baima gabbro is platinum-subgroup PGE (PPGE = Rh, Pt and Pd) enriched and iridium-subgroup PGE (IPGE = Os, Ir and Ru) depleted, with a distinct positive Ru anomaly on a primitive mantle normalized multi-element plot. The Taihe gabbros are also PPGE enriched but with negative Ru and Pd anomalies on a primitive mantle normalized multi-element plot. The PGE concentrations of Baima rocks are indicative of fractionation of a relatively evolved, mafic, S-undersaturated parental magma that was affected by earlier sulphide segregation. In contrast, the Taihe rocks record evidence of both S-saturated and S-undersaturated conditions and that the parental magma was likely emplaced very close to S-saturation. Comparisons of the platinum group element contents in the Emeishan flood basalts and the Emeishan oxide-bearing intrusions suggest that the PGE budget in a magma is not controlled by magma series (high-Ti vs. low-Ti), but very much by crustal contamination. The unlikelihood of substantial crustal contamination in the Taihe magma allowed the magma to remain S-undersaturated for a longer duration. PGE and sulphide mineralization was not identified in the Taihe intrusion but the presence of one PGE-enriched sample (Pt + Pd = ~300 ppb) suggests that the parental magma likely did not experience sulphide segregation and is a potential target for further prospecting.

1. Introduction

The Late Permian Emeishan large igneous province (ELIP) of SW China is host to magmatic Ni–Cu–(PGE) sulphide and Fe–Ti–V oxide deposits which contain economic to subeconomic concentrations of metals (Zhou et al., 2008). The formation of a given deposit-type (i.e. sulphide vs. oxide) is thought to be related to the type of parental magma (i.e. high-Ti basalt vs. low-Ti basalt) and the subsequent processes (i.e. fractional crystallization and sulfur segregation) which allowed for metal enrichment (Zhong et al., 2002, 2003, 2004; Song et al., 2003, 2008; Wang et al., 2006, 2007, 2010; Zhou et al., 2008; Shellnutt et al., 2011; Shellnutt and Wang, 2014). There are at least five (e.g. Baima, Hongge, Panzhihua, Taihe and Xinjie) mafic-ultramafic intrusions located within the central part of the inner zone of the ELIP which contain significant oxide and to a lesser extent sulphide deposits. The Panzhihua, Baima and Taihe deposits are hosted within evolved layered gabbroic intrusions which are primarily oxide-rich whereas the Hongge and Xinjie deposits are hosted within layered mafic-ultramafic intrusions which are sulphide and oxide-rich.

* Corresponding author. Tel.: +886 2 7734 6386; fax: +886 2 2933 3315.
E-mail addresses: jgshelln@ntnu.edu.tw, gshellnutt@hotmail.com (J.G. Shellnutt).

http://dx.doi.org/10.1016/j.chemer.2014.06.002
0009-2819/

The enrichment of metals within the Panzhihua, Baima and Taihe oxide-bearing intrusions is debated and is thought to be due to a number of factors including: 1) Fe-rich picritic parental magmas (Zhang et al., 2009; Hou et al., 2012), 2) silicate liquid immiscibility (Zhou et al., 2005, 2013), 3) assimilation of carbonate rocks (Ganino et al., 2008) or 4) fractional crystallization (Shellnutt et al., 2009, 2011; Shellnutt and Jahn, 2010). As a consequence of their oxide-rich nature, the Panzhihua, Baima and Taihe intrusions have not been considered to be primary targets for platinum group element prospecting. However, Maier et al. (2003) documented PGE-rich horizons within the oxide-rich Stella intrusion of South Africa and suggested that some oxide-rich deposits may indeed contain economic concentrations of PGEs. As well, in other mafic–ultramafic intrusions, such as the Lac des Iles Intrusive Complex, Canada, migration of deuteric fluids has been considered as an important process contributing to PGE, particularly Pd, mineralization within the intrusion. Furthermore, the behavior of PGEs provides valuable insight for the effects of crystal fractionation of sulphides and silicate minerals within a magma system. Chalcophile elements, such as the PGEs, Ni and Cu, have extremely high sulphide–silicate partition coefficients, of which those for the PGEs are at least an order of magnitude higher than for Ni or Cu, making the chalcophile elements useful proxies for sulphide fractionation in the parental magma (Keays, 1995; Maier and Barnes, 1999; Maier et al., 2003; Crocket and Paul, 2004; Lightfoot and Keays, 2005). For instance, a magma undergone sulphide fractionation is expected to be highly depleted in PGEs relative to Ni and Cu, thus high in Cu/Pd and Ni/Ir.

In order to understand the behavior of sulfur and to determine the likely S-conditions of their parental magmas in the Baima and Taihe magmatic systems, we present platinum group element analyses of these rocks. We also compare our new results with previously published work from the other PGE-bearing cumulate rocks (i.e. Xinjie, Hongge) of the ELIP in order to determine if there are similarities between the two different types of magmatic oxide deposits in the Panxi region.

2. General geology

The Emeishan large igneous province (ELIP) covers an area of 0.3×10^6 km^2 within southwestern China and northern Vietnam and consists of flood basalts, spatially associated felsic plutons and layered mafic–ultramafic intrusions, some of which host giant Fe–Ti–V oxide or Ni–Cu sulphide deposits (Fig. 1a; Chung and Jahn, 1995; Ali et al., 2005; Wang et al., 2007; Zhou et al., 2008; Shellnutt, 2014). The ELIP is located along the western edge of the Proterozoic Yangtze Block near the boundary with the Early Triassic Songpan-Ganze terrane and was subsequently dismembered during the Mesozoic and Cenozoic by post-emplacement faulting associated with the collision of the North China Block and South China Block and the Indo-Eurasian collision (Chung and Jahn, 1995; Liu et al., 2006). The volcanic succession includes picrites, basaltic andesites, rhyolites, trachytes and basalts which range in composition from tholeiitic to transitional (Xu et al., 2001; Xiao et al., 2004; Wang et al., 2007; Fan et al., 2008; Shellnutt and Jahn, 2011). The basalts form the most voluminous rock type and range in thickness from 1.0 to 5.0 km in the western part and 0.2 to 2.6 km in the eastern part. A mantle-plume model is ascribed to explain the geological features of the ELIP such as the extensive flood basalts, ultramafic lavas, short eruptive duration (260–257 Ma), structural doming and lower crustal seismic velocity layers and is considered to have contributed to the decline in biota during the end-Guadeloupian mass extinction (Xu et al., 2004; Ali et al., 2005; He et al., 2007; Shellnutt et al., 2012; Shellnutt, 2014). Although ELIP magmatism was short lived, Emeishan-related underplated mafic rocks probably served as a source for mafic and felsic magmas after emplacement (Xu et al., 2008; Shellnutt et al., 2008, 2012).

The Panxi region, between the cities of Panzhihua and Xi Chang, of southern Sichuan province is an important area within the ELIP because plutonic and hypabyssal rocks are exposed including mafic–ultramafic intrusions which host substantial orthomagmatic Fe–Ti–V oxide deposits. The Panzhihua, Baima and Taihe gabbros are chemically evolved and spatially associated with peralkaline granitic rocks whereas the Hongge and Xinjie intrusions are predominantly ultramafic suggesting there are petrogenetic differences between the two types of intrusions (Shellnutt and Zhou, 2007; Zhang et al., 2009; Tao et al., 2010; Shellnutt et al., 2011; Shellnutt and Wang, 2014).

The Baima igneous complex (BIC) is located in the central part of the Panxi region (Fig. 1c), ~100 km northeast of Panzhihua, and consists of gabbroic and syenitic units (Chen, 1990; Yang et al., 1997; Shellnutt et al., 2009). The layered gabbroic unit lies to the east of the syenitic unit and is dipping ~25° to the west and contains cumulus olivine, clinopyroxene and plagioclase with interstitial oxide minerals (Shellnutt and Pang, 2012). The U/Pb zircon ages of the two units are within error of ~260 Ma and cover an area of similar size, but their respective volumes are unknown (Shellnutt et al., 2009). Samples were collected at surface exposures across the northern portion of the intrusion (Fig. 1c). The syenitic unit is structurally above the gabbroic unit and contains abundant ellipsoidal mafic enclaves varying in size from a few centimeters to tens of centimeters in length (Shellnutt et al., 2010).

The Taihe layered gabbroic intrusion is located to the west of the city of Xi Chang and is currently being mined for Fe–Ti–V oxide minerals (Fig. 1d). Samples were collected at two localities and the rocks have similar textures and mineralogy as the Baima rocks (Shellnutt et al., 2011). The first group of samples (GS04-159 to -165) was collected from the central portion of the open pit whereas the second group of samples (GS04-170 to -173) was collected ~100 m to the east. To the east of the gabbroic intrusion is the Taihe peralkaline granite which is exposed in a series of quarries in the surrounding highland. The peralkaline granite and layered gabbro have U/Pb zircon ages of ~260 Ma and the entire complex is fault bound with basalts (Xu et al., 2008). Similar to the Baima peralkaline syenites, the granitic pluton contains numerous microgranular enclaves (Shellnutt et al., 2010).

3. Petrography

3.1. Baima gabbros

The Baima layered gabbro consists of four main lithological zones, with increasing stratigraphic height: the lower cumulate zone, oxide ore zone, olivine gabbro zone and upper gabbro zone (Chen, 1990; Shellnutt and Pang, 2012). The gabbros consist of variable proportions of coarse grained cumulate olivine, plagioclase, clinopyroxene and interstitial Fe–Ti oxide minerals with minor amounts of sulphide minerals, Fe–Mg spinel and apatite. The olivine is typically rounded and ranges in size from a few millimeters (~5 mm) to <0.1 mm. It decreases in abundance from ~30% in the lower cumulate zone to <5% in the upper gabbro zone whereas the pyroxene makes up a larger portion of the mode toward the upper parts of the complex. The plagioclase is commonly tabular, euhedral to anhedral in shape and ranges in size from ~5 mm to <0.1 mm and has alteration rims of brown hornblende or biotite when in contact with oxide minerals. The clinopyroxene appears similar in size and shape to the plagioclase crystals and is pleochroic with extensive ilmenite exsolution lamellae. The oxide minerals are primarily made of an interstitial network surrounding the silicate minerals. The magnetite displays extensive oxidation exsolution lamellae of

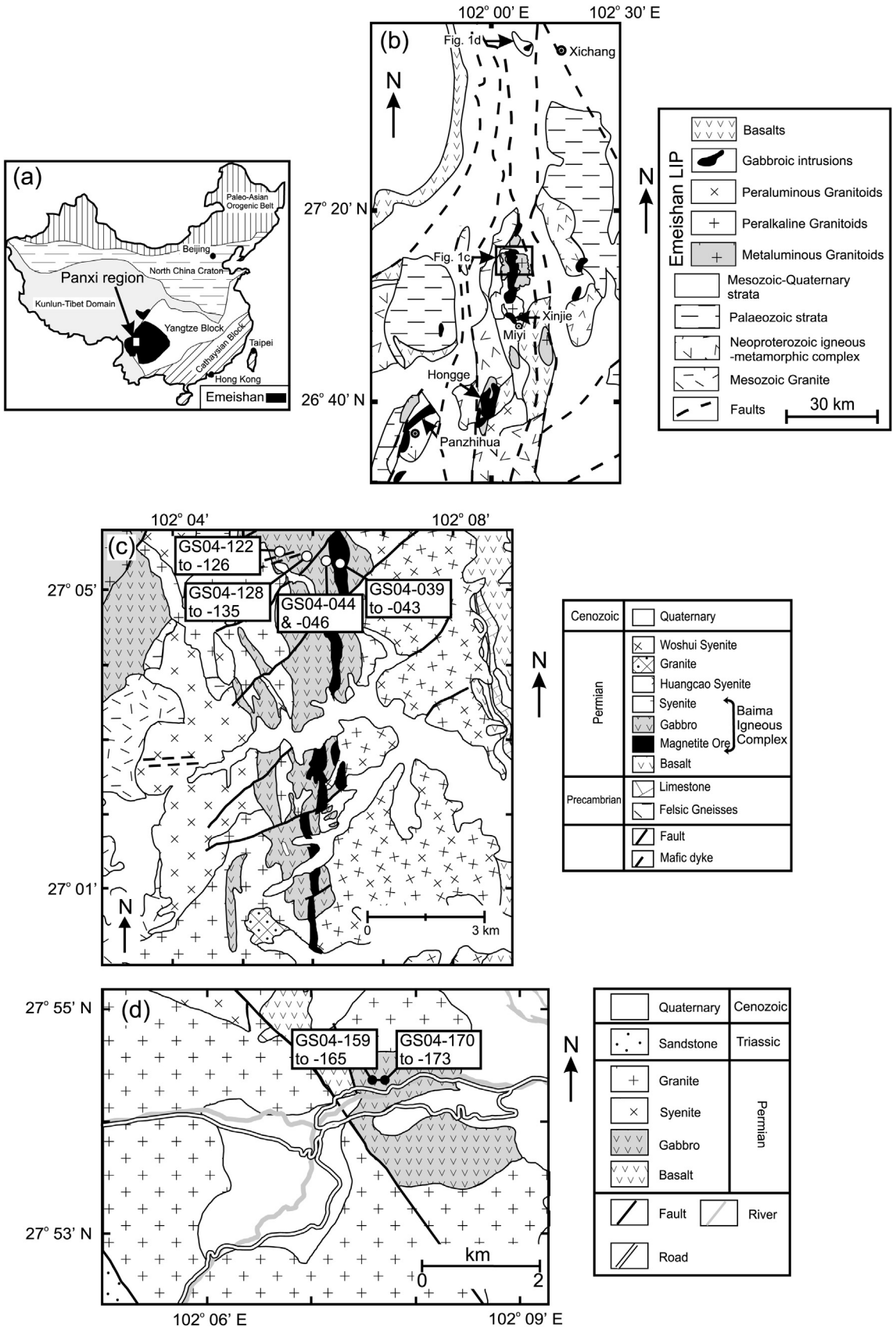

Fig. 1. (a) Location of the Panxi region of the Emeishan large igneous province. (b) Location of Baima and Taihe igneous complexes. (c) Geological map of the Baima region surrounding rocks including the sampling localities (modified from Wang et al., 1994). Samples GS04-039 to -043 from the oxide ore zone (OXZ); samples GS04-044 to -046 from the olivine gabbro zone (OGZ); samples GS04-128 to -135 from the olivine gabbro zone (OGZ); samples GS04-122 to -126 from the upper gabbro zone (UGZ). (d) Geological map of the Taihe complex including the sampling localities (modified from Wang et al., 1993).

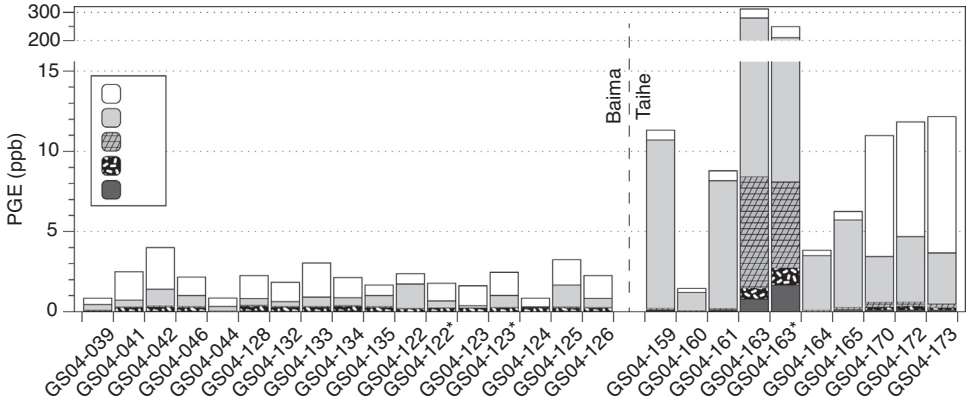

Fig. 2. Histograms of the elemental and bulk PGE content of the Baima and Taihe gabbroic intrusions.

ilmenite and spinel usually along 120° triple junction grain boundaries. The ilmenite becomes the most abundant oxide mineral in the upper gabbro zone whereas spinel disappears. The apatite is typically an accessory mineral and rarely exceeds ~0.5 vol.% below the upper gabbro zone, however within the upper gabbro zone it can be as much as ~5 vol.%. Sulphide (i.e. pyrite and chalcopyrite) minerals are generally not that common however they are more abundant within the olivine gabbro zone and most often associated as amorphous blebs within the interstitial oxide minerals.

3.2. Taihe gabbros

The gabbroic rocks consist of variable proportions of coarse grained cumulus olivine, plagioclase, clinopyroxene, interstitial oxide and sulphide minerals and apatite. The mineral modes for the olivine gabbros and gabbros are generally defined as olivine ≤10%, plagioclase 45% and 55%, clinopyroxene 20 and 35% and oxide minerals are ≤10% in the silicate-rich samples. The Fe–Ti oxide ores contain ≤10% silicate minerals and ≥90% spinels and ilmenite. The olivine crystals are a few millimeters in size (<2 mm) and tend to have rounded shapes. The plagioclase typically forms tabular, euhedral to anhedral crystals and tend to have rims of brown hornblende or biotite when in contact with oxide minerals. The clinopyroxene crystals are similar in size and shape to the olivine crystals and many have oxide exsolution lamellae of ilmenite. The oxide minerals (i.e. magnetite, ilmenite and spinel) are interstitial to the silicate minerals and tend to form a net-texture. The principal oxide mineral is magnetite followed by ilmenite. Spinel (i.e. pleonaste and chromite) and ilmenite are commonly present as oxidation exsolution lamellae within the magnetite. The sulphide minerals (i.e. pyrite and chalcopyrite) tend to be included within the interstitial oxides and apatite is relatively rare and rarely exceeds 0.5%. Scanning electron microprobe (SEM) screening reveals minute grains of Pt–Te alloys, Ag–Pd alloys, Ag–bearing sulphides, and Se-bearing sulphides enclosed within silicates or oxides.

4. Methods

Powdered samples, prepared using an agate mill, were digested with aqua regia in a 75 ml Carius tube. An appropriate amount of enriched isotope spike solution containing ^{194}Pt, ^{105}Pd, ^{101}Ru, and ^{193}Ir were accurately added and mixed with aqua regia. The sealed Carius tube was placed in a custom-made high-pressure autoclave filled with water to prevent explosion of the tube when heated to about 300 °C (Qi and Zhou, 2008; Qi et al., 2007). After 10 h, the Carius tube was cooled and the contents were transferred to a 50 ml centrifuge tube. After centrifuging, the upper solution was transferred to a distillation system (Qi and Zhou, 2008). After distillation, the solution was used to pre-concentrate PGEs by Te-coprecipitation and all the interference elements are removed by using a cation exchange resin and P507 extraction chromatography resin combined in the same column as described by Qi et al. (2004).

Platinum, Pd, Ru, and Ir were measured by isotope dilution (ID)-inductively coupled plasma mass spectrometry (ICP-MS). The mono-isotope element Rh was measured by external calibration using a ^{194}Pt spike as the internal standard (Qi et al., 2004). The instrument used in this study is an VG PQ ExCell ICP-MS at The University of Hong Kong. The total procedural blanks were lower than 0.003 ng/g for Re, Ru, Rh and Ir; 0.020 ng/g for Pd; and 0.011 ng/g for Pt. The results of reference standards WPR-1 (peridotite) and UMT-1 (ultramafic ore tailings PGE material) are listed in Table 1. The mass bias effect was externally monitored using a 10 ng/ml natural Ru, Ir, Pd and Pt standard solution determined during the course of the measurement and corrected with linear interpolation of the measured ratio of the standard solution against the reference value (IUPAC, 1991). The results for WPR-1 are in agreement with the certified values.

5. Results

The samples from Baima gabbroic rocks have low total PGE abundances (ΣPGE < 4 ppb). Palladium and Pt are the most abundant elements which form 71% to 96% of the total PGE abundance (Figs. 2 and 3, Table 1) whereas concentrations of Ir and Rh are very low, generally ≤0.05 ppb while Ru is higher (≤0.32 ppb). The Ni (21–333 ppm), Cr (12–130 ppm), Cu (26–579 ppm), Zr (6–16 ppm) and MgO (4.0–13.4 wt%) contents are variable and reflect relative proportions of cumulate silicates to oxides. The PGE abundances are not correlated with Cr, Ni, Cu, Zr (not shown) and MgO (Fig. 4).

The Taihe gabbroic rocks have variable total PGE abundances ranging from ΣPGE < 2 ppb to ΣPGE ~300 ppb however most samples have ΣPGE ~10 ppb (Fig. 2). The PGE concentrations of the Taihe gabbros are more than double the concentration of the Baima gabbros. The samples (e.g. GS04-170, -172, -173) from the eastern part of the outcrop have similar concentrations with low Pt/Pd ratios (Pt/Pd = 0.4–0.6) whereas the samples from the western part have variable concentrations and higher Pt/Pd ratios (Pt/Pd = 4.6–16.9) (Fig. 5). The Ni (63–427 ppm), Cr (32–621 ppm), Cu (129–1255 ppm), Zr (11–60 ppm) and MgO (4.0–6.3 wt%) contents are generally similar to the Baima gabbroic rocks and reflect the difference in the modal proportions of the constituent cumulus minerals.

The primitive mantle normalized plots show very distinct patterns for the Baima and Taihe gabbros (Fig. 6). The Baima gabbros show PPGE (PPGE = Rh, Pt and Pd) enrichment over the IPGEs (IPGE = Os, Ir and Ru) however there are distinct positive anomalies of Ru. The positive Ru anomalies are unusual for mafic rocks but are reported for ultramafic rocks in particular peridotites (e.g. dunites and harzburgites; Zhou et al., 1998; Buchl et al., 2004). It is also possible that positive Ru anomalies are an analytical artifact of excess Ni argides (^{101}Ru = ^{61}Ni + ^{40}Ar; e.g. Park et al., 2012a), however we are more inclined to the geological interpretations of this feature because (1) such anomalies are not correlated with Ni in the Baima samples (indeed the positive ones are those characterized by modest to low Ni abundances), and (2) our analytical method was

Table 1
Whole rock platinum group element chemical analyses of the Taihe and Baima layered gabbros.

Sample	Location	Ru (ppb)	Pd (ppb)	Ir (ppb)	Pt (ppb)	Rh (ppb)	ΣPGE	MgO (wt.%)	TiO_2 (wt.%)	Cr (ppm)	Ni (ppm)	Cu (ppm)	Zr (ppm)	Y (ppm)	Yb (ppm)	Th (ppm)
Taihe																
GS04-159	Gabbro	0.01	0.62	0.08	10.50	0.11	11.32	5.81	2.73	94	146	244	60	7.7	0.68	1.63
GS04-160	Gabbro	0.01	0.25	0.02	1.15	0.02	1.45	5.38	2.88	32	69	129	30	8.1	0.63	0.77
GS04-161	Gabbro	0.02	0.63	0.06	7.98	0.10	8.79	3.95	2.91	82	192	441	19	6.4	0.51	0.31
GS04-163	Ore	0.70	31.63	0.80	271.61	6.90	311.64	6.32	2.95	621	427	1255	11	1.1	0.07	0.06
GS04-163[a]	Ore	1.08	39.65	1.66	201.58	5.35	249.32									
GS04-164	Gabbro	n.d.	0.34	0.04	3.42	0.04	3.84	5.00	2.87	68	102	242	23	5.8	0.40	0.31
GS04-165	Gabbro	0.01	0.52	0.14	5.47	0.10	6.24	4.65	2.92	89	143	247	18	5.5	0.41	0.30
GS04-170	Gabbro	0.20	7.53	0.10	2.87	0.28	10.98	6.14	2.25	122	106	122	13	5.2	0.40	0.13
GS04-172	Gabbro	0.24	7.16	0.11	4.07	0.25	11.83	5.01	1.29	90	63	47	16	5.6	0.46	0.41
GS04-173	Gabbro	0.16	8.49	0.10	3.19	0.22	12.16	5.51	2.63	111	109	131	13	4.7	0.38	0.15
Baima																
GS04-122	UGZ	0.19	0.65	n.d.	1.53	0.01	2.38	5.69	4.46	29	31	62	10	6	0.48	0.10
GS04-122[a]	UGZ	0.21	1.10	0.02	0.44	0.01.	1.78									
GS04-123	UGZ	0.24	1.45	0.01	0.75	0.01	2.46	5.58	4.72	31	31	60	11	6	0.52	0.11
GS04-123[a]	UGZ	0.21	1.24	0.01	0.16	n.d.	1.62									
GS04-124	UGZ	0.23	0.55	0.01	0.05	0.01	0.85	5.84	4.44	28	31	54	10	11	0.68	0.21
GS04-125	UGZ	0.21	1.59	0.03	1.38	0.04	3.25	3.70	1.45	65	39	26	7	5	0.37	0.07
GS04-126	UGZ	0.21	1.42	0.03	0.58	0.02	2.26	3.98	3.48	12	21	42	11	9	0.58	0.27
GS04-128	OGZ	0.32	1.43	0.04	0.44	0.02	2.26	8.21	5.36	86	133	171	7	2	0.15	0.09
GS04-132	OGZ	0.28	1.21	0.02	0.31	0.02	1.84	8.12	3.04	29	91	108	6	3	0.23	0.18
GS04-133	OBZ	0.28	2.12	0.02	0.60	0.02	3.04	4.14	2.43	45	70	107	8	4	0.24	0.22
GS04-134	OGZ	0.31	1.26	0.04	0.49	0.03	2.13	7.97	4.44	73	132	183	6	2	0.14	0.09
GS04-135	OXZ	0.26	0.66	0.02	0.69	0.03	1.66	13.43	6.43	109	184	234	8	3	0.26	0.06
GS04-039	OXZ	0.02	0.40	0.05	0.36	0.02	0.85	10.72	9.22	116	333	579	10	2	0.22	0.03
GS04-041	OXZ	0.25	1.77	0.02	0.44	0.02	2.50	11.14	8.87	116	121	195	12	2	0.19	0.02
GS04-042	OXZ	0.28	2.59	0.03	1.05	0.05	4.00	9.16	8.58	130	178	511	10	1	0.11	0.03
GS04-044	OXZ	n.d.	0.53	0.02	0.30	0.01	0.86	6.19	4.11	27	42	67	12	4	0.25	0.02
GS04-046	OGZ	0.25	1.17	0.03	0.69	0.03	2.17	4.69	2.23	62	38	52	16	7	0.47	0.21
UMT-1		11.06	171.98	8.89	124.54	9.22										
UMT-1 (r.v.)		10.9	106	8.8	129	9.5										
WPR-1		23.26	244.13	12.38	295.85	12.40										
WPR-1 (r.v.)		21.6	235	13.5	285	13.4										

[a] Duplicate samples. UMT-1 and WPR-1 are measure standard reference materials. The MgO, TiO_2, Cr, Ni, Cu and Zr data from Shellnutt et al. (2009, 2011). r.v.: recommended value; UGZ: uppger gabbro zone; OGZ: olivine gabbro zone; OXZ: oxide ore zone.

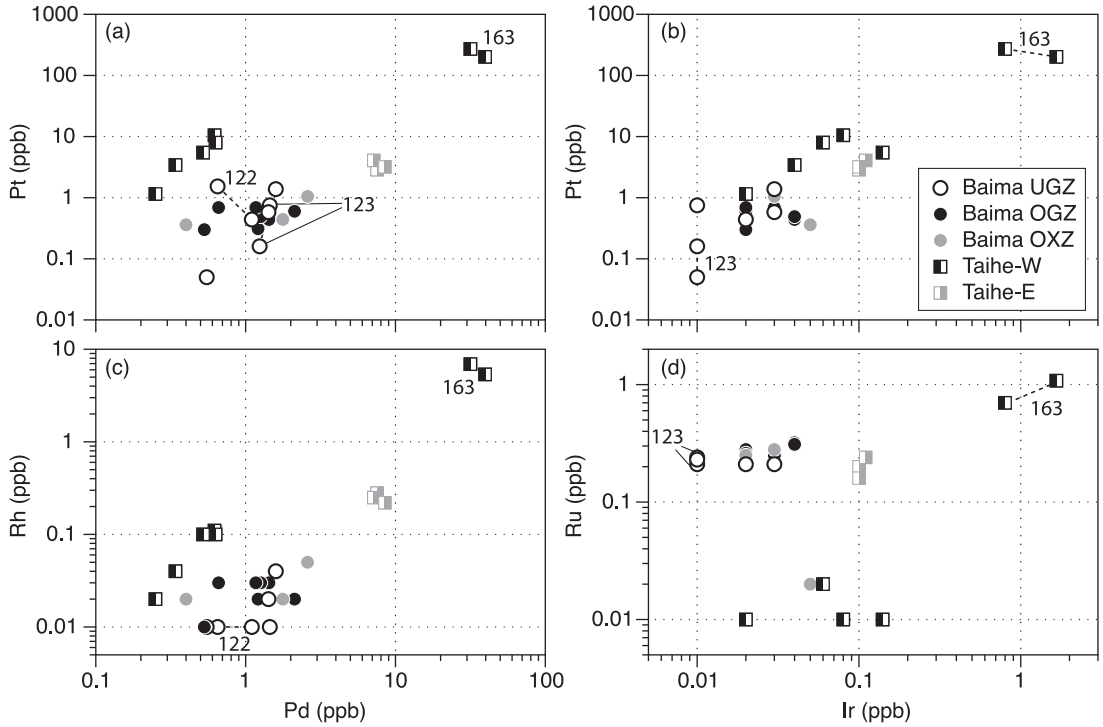

Fig. 3. (a) Pt vs. Pd, (b) Pt vs. Ir, (c) Rh vs. Pd and (d) Ru vs. Ir for the Baima and Taihe intrusions. Note the reasonable correlations for samples from the western part of the Taihe intrusion. The loss of correlation in Ru vs. Ir may be an artifact of rounding to two decimal places. Duplicate analyses of the same samples are connected by dashed lines.

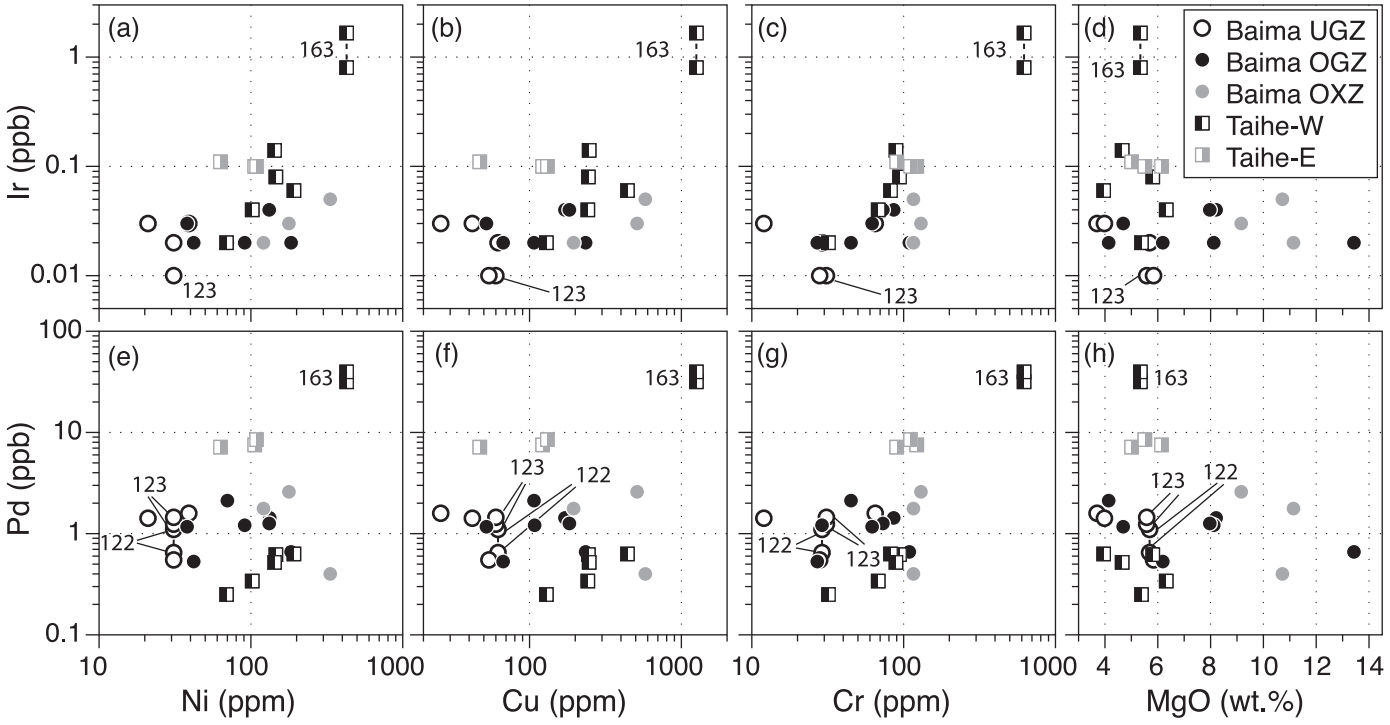

Fig. 4. Selected PGE (Ir and Pd) vs. Ni, Cu, Cr and MgO. Note the weak correlations among PGE, Ni, Cu and Cr for the samples from the western portion of the Taihe intrusion. Duplicate analyses of the same samples are connected by dashed lines.

designed such that Ni and other potentially interfering elements are filtered out before measurement (see Section 3).

Perhaps the most striking feature of the Taihe gabbro is that of its zoned PGE spider patterns observed within a single intrusion, strongly suggesting that the PGE variations in the intrusion are a result of magma evolution, rather than a source feature. Samples collected from the eastern part of the pluton are almost identical in concentrations and characterized by a smooth pattern with high Pd/Ir (Fig. 6f). Those from the western part are characterized by an irregular pattern with extreme superchondritic Ir/Ru and Pt/Pd and highly variable concentrations (Fig. 6e).

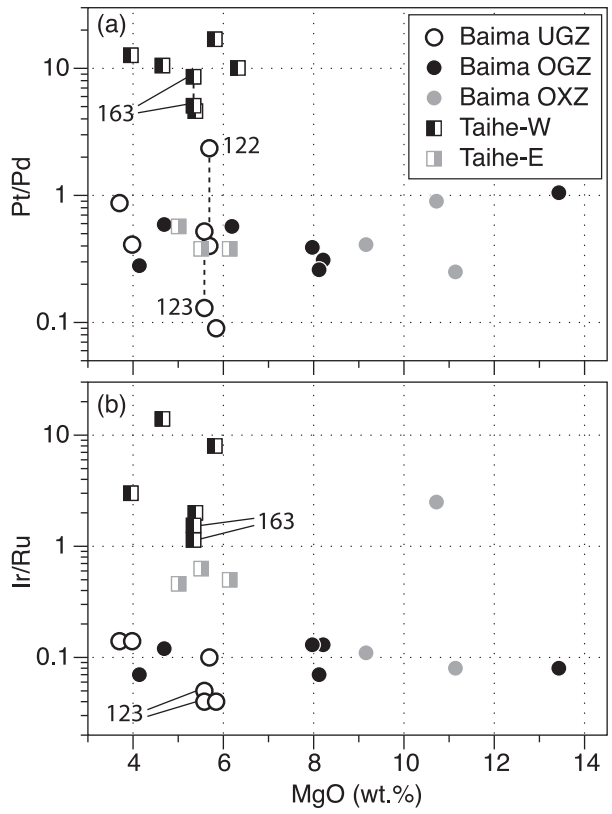

Fig. 5. (a) Pt/Pd and (b) Ir/Ru vs. MgO for the Baima and Taihe intrusions. Duplicate analyses of the same samples are connected by dashed lines.

6. Discussion

6.1. Fractional crystallization and sulfur saturation

Determining the state of S-saturation and whether sulphide segregation has occurred in a suite of intrusive rocks is crucial to understanding the distribution of PGEs and formation of layered ore deposits, owing to the extremely high sulphide liquid–silicate liquid partition coefficients for PGEs and other chalcophile elements (e.g. Barnes and Maier, 1999; Naldrett, 2010). Direct measurement of S-contents in samples may be insightful, but has in many cases been considered unreliable because of the volatile and mobile nature of S which is lost during magma degassing or low-temperature alteration (Andersen, 2006; Zhong et al., 2011a; Bai et al., 2012; Naldrett et al., 2012). Gauging the state of sulphide fractionation is possible, nevertheless, by comparing the concentrations of PGEs and other chalcophile elements, such as Ni and Cu. In particular, Ni/Ir, Cu/Pd and Cu/Zr are very useful, because these element pairs have similar compatibility between silicate liquids and major rock-forming minerals if sulphides are not present, but Ir, Pd and Cu are strongly partitioned into sulphide phases compared to Ni, Cu and Zr, respectively, under S-saturated conditions. If the sulphides are segregated from the silicate magmas, elevated Ni/Ir, Cu/Pd and low Cu/Zr would be resulted in the residual chalcophile-depleted magmas.

6.1.1. Baima gabbros

The Baima gabbros have very high Cu/Zr (3.3–58) and Cu/Y (5–290) ratios, compared to ~2–3 and 5–7, respectively, in the primitive mantle (McDonough and Sun, 1995; Palme and O'Neill, 2003). Although they are poor in Zr, the high Cu/Zr ratios may arguably reflect the partitioning of Zr into the felsic portions of the igneous complexes (Fig. 7) (Shellnutt et al., 2009, 2011), the high Cu/Zr and Cu/Y ratios are positively correlated with the Cu content (26–579 ppm), more likely reflecting accumulation of sulphides in the gabbros to some degree. In contrast, $(Cu/Pd)_N$ (2.3–205; Fig. 8a), $(Ni/Ir)_N$ (1.2–16; Fig. 8f) and HFSE/PPGE [e.g. $(Y/Pt)_N = 1.5–352$; Fig. 8k] are high in the Baima gabbros [subscript N denotes normalization by primitive mantle values of Barnes and Maier (1999) and Y value of McDonough and Sun, 1995)] which also have low ΣPGE abundances (0.9–4.0 ppb), suggesting that the accumulated sulphides are of low PGE varieties and that the PGEs must have been stripped off during an earlier episode of S-saturation or retained in the mantle as a result of low degrees of partial melting (e.g. Keays, 1995) or melting under a low fO_2 condition (Mungall et al., 2006). The high HFSE/PPGE ratios are considered to indicate the removal of PPGEs (e.g. Pt), but not HFSEs (e.g. Y), during sulphide segregation, which otherwise are not significantly different in silicate partitioning in the absence of a sulphide phase (Brügmann et al., 1993). On the plot of $(Cu/Pd)_N$ vs Pd (Fig. 9a; see also Barnes and Maier, 1999), the Baima gabbros clearly fall into the "depleted" side of the diagram, with low Pd and high $(Cu/Pd)_N$, typical of magmas (e.g. the Hongge intrusion; Bai et al., 2012) that experienced sulphide fractionation. As a sulphide-fractionation vs -accumulation "discrimination" diagram, it is compelling in that once a magma has reached sulphide saturation, the PGEs are so strongly partitioned into the sulphide phase that the magma would become PGE-barren. If the resultant magma subsequently reaches S-saturation again and somehow trapped some of such sulphides in the cumulates, the rock would still fall into the "depleted" side of the $(Cu/Pd)_N$–Pd diagram, because the cumulus sulphides would inherit the PGE-poor (high Cu/Pd) nature of the magma from which they precipitate out, unlike rocks that initially reached sulphide saturation and accumulated the PGE-rich sulphides very early in their magmatic differentiation (e.g. the Xinjie intrusion; Zhong et al., 2011a). On the same plot (Fig. 9a), the amount of sulphide fractionation (segregation in the crust or retention in the mantle) can be gauged from the magnitude of $(Cu/Pd)_N$ deviates from a primitive magma, here assumed as the average of Emeishan picrites (data of Li et al., 2012 and their compilation, with additional data from Wang et al., 2007). There, most of the Baima samples can be explained by a small amount of sulphide segregation, <0.01% sulphide, if $D_{Pd}^{\text{sulphide liq./silicate liq.}} = 25{,}000$ and $D_{Cu}^{\text{sulphide liq./silicate liq.}} = 1000$ (Naldrett, 2010). Two samples with substantially higher $(Cu/Pd)_N$ require segregation of less than 0.02% sulphide. Note that these values can only be regarded as maximum estimates, because the gabbros may have been affected by some sulphide accumulation.

In conjunction with their high mantle-normalized values, Cu/Pd, Ni/Ir and Y/Pt, despite some scatter, positively correlate with MgO, Ni, Cu, TiO_2 and to a lesser extent Cr in the Baima gabbros and display systematic variations through the stratigraphy (Fig. 8a–o). For instance, $(Cu/Pd)_N$ are highest in the oxide ore zone (16–206), suggestive of sulphide depletion, and lowest in the upper gabbro zone (2.3–14), suggestive of sulphide bearing. The samples from the olivine gabbro zone have a large range [$(Cu/Pd)_N = 6.3–50$] but are in general intermediate between the oxide ore zone and upper gabbro zone (Fig. 8a–e). The Pd concentrations do not show a systematic change from the oxide ore zone to the upper gabbro zone however the Cu concentration systematically decreases leading to the change in the Cu/Pd ratios (Figs. 7 and 8a). Likewise, the Pd/Cr ratios increase from the lower regions (3×10^{-6} to 2×10^{-5}) to the upper parts (2.3×10^{-5} to 1.1×10^{-4}), and negatively correlate with MgO, Ni, Cr, Cu and TiO_2 (Fig. 8p–t). Sulphide fractionation alone is unlikely to produce these observed variations, because it would not have affected MgO and TiO_2. These variations are more likely due to concurrent fractionation of silicate minerals and sulphides, and possibly ilmenite, magnetite and chromite, up section or accumulation down section. Given that the Baima gabbros are

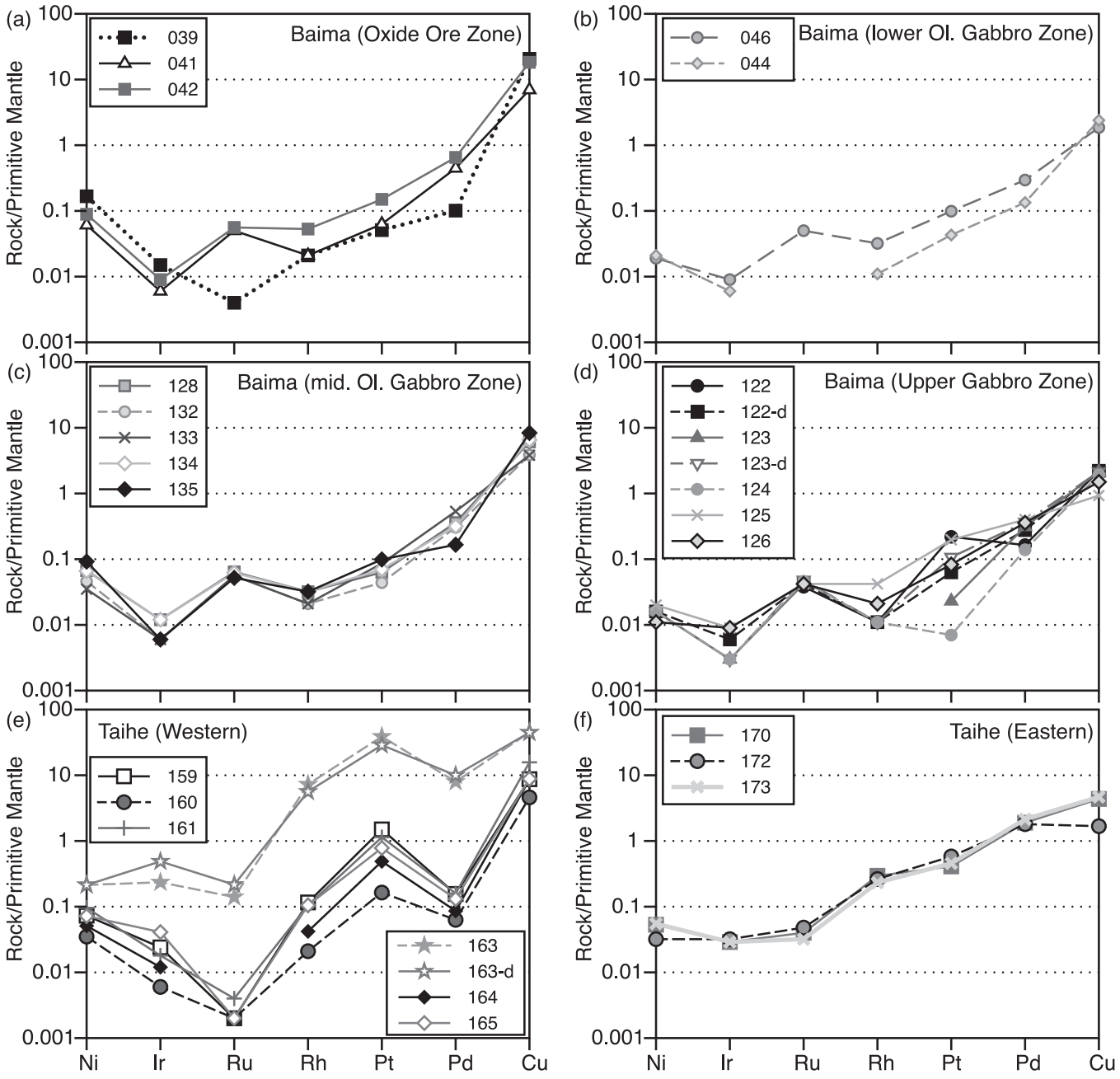

Fig. 6. Primitive mantle normalized chalcophile-element multi-element plots for the (a-d) Baima and (e and f) Taihe oxide-bearing gabbroic intrusions. d- denotes duplicate analysis. Primitive mantle normalizing values are from Barnes and Maier (1999).

characterized by positive Ru anomalies and Ru is substantially more compatible than Ir and Rh in chromites (Puchtel and Humayun, 2001; Brenan et al., 2012; Pagé et al., 2012; Park et al., 2012b), the Baima gabbros likely reflect accumulation of chromites at least to some degree. As suggested above, the Baima parental magma had been saturated with sulfur before the differentiation occurred, and much of its PGE had been either lost to the segregated sulphides at depth or retained in the mantle. Perhaps as a result of decompression during upwelling that increased the solubility of sulphide in the magma (Mavrogenes and O'Neill, 1999), the magma became S-undersaturated. However, this would not last long as the magma continued crystallizing. Sulfur content at sulphide saturation (SCSS) is controlled by a combination of such factors as temperature, pressure and magma composition, in particular FeO; the higher the FeO of a magma, the higher the SCSS (O'Neill and Mavrogenes, 2002). In Baima, the compositional stratigraphy (Cu/Pd and Pd/Cr vs. MgO, TiO_2, Ni, Cr and Cu correlations and decreasing Cu/Pd as well as increasing Pd/Cr up section from oxide ore zone to the upper gabbro zone) strongly suggests that the crystallization of the Fe-oxides triggered sulphide segregation by reducing the SCSS, and sulphides are accumulated down section in the oxide ore zone and to a lesser extent the intermediate olivine gabbro zone.

6.1.2. *Taihe gabbros*

Samples collected from the eastern part of the pluton have almost identical PGE concentrations and are characterized by a smooth pattern with high Pd/Ir (Fig. 6f). The PGEs of those from the western part are characterized by an irregular pattern with extreme superchondritic Ir/Ru and Pt/Pd and highly variable concentrations (Fig. 6e). The smooth PGE pattern of the eastern

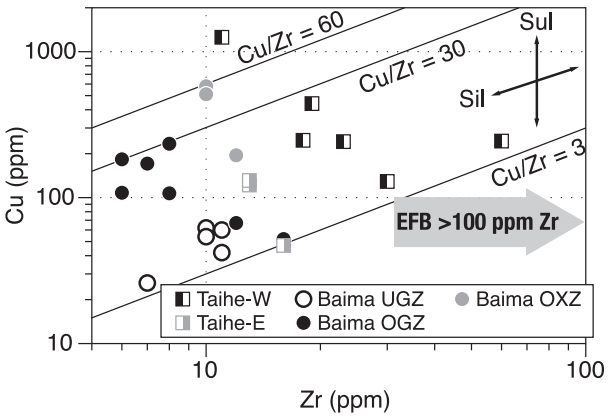

Fig. 7. Cu vs. Zr for the Baima and Taihe intrusions. Thin vectors indicate theoretical sulphide (sul) and silicate (sil) controls of these elements, and the thick arrow denotes the high Zr contents (>100 ppm) for typical Emeishan flood basalts (EFB).

samples in conjunction with their near-unity mantle-normalized Ni/Ir and Cu/Pd (Fig. 6a–j) suggest that the magma did not undergo substantial sulphide segregation, neither in the crust nor in the mantle during partial melting. The sulphides observed under the microscope occur as an intercumulus phase occupying the interstitial positions among the silicates and oxides, suggesting that S-saturation occurred late in the differentiation history of the intrusion. Accordingly, some of the PGE variations in the eastern gabbros must be controlled by the early crystallizing silicates, spinels and Fe–Ti oxides. The fractionated PPGE/IPGE pattern of these samples is consistent with removal of IPGEs by olivine ± chromite ± Fe–Ti oxide fractionation.

In contrast, the western samples exhibit variable and generally high $(Cu/Pd)_N$ (4.5–101), suggestive of prior sulphide removal. On the $(Cu/Pd)_N$–Pd plot (Fig. 9a), the data cluster in two groups with one group (the majority of the western samples) having low Pd and high $(Cu/Pd)_N$ which may be explained by segregation of 0.012–0.015% sulphides and another (the two analyses of the same oxide-rich sample (GS04-163) having very high Pd and low $(Cu/Pd)_N$ which may suggest sulphide accumulation. However, the very high Pt/Pd and Ir/Ru in the Taihe gabbros need further explanation. Except that of the PGE-rich sample GS04-163, the Pt/Pd in the Taihe western gabbros positively correlate with Pt, suggesting that this ratio may be controlled by selective enrichment of Pt, instead of depletion had sulphide fractionation occurred. In other words, the magma from which sulphides have been fractionated would have had high Pt/Pd and low Pt, possibly due to the slightly higher Pd partitioning in the sulphide liquids (Fleet and Stone, 1991; Peach et al., 1994; Vogel and Keays, 1997). Likewise, the very high Pt/Pd in the sulphide-bearing GS04-163 may also reflect Pt enrichment because sulphide accumulation would have resulted in low Pt/Pd.

Among the Taihe western samples, the PGEs are positively correlated with each other to some degree (Fig. 3), and with Cr, Cu, Co and Ni (Fig. 4), consistent with co-precipitation of sulphides with silicates or oxides. Conversely, no chalcophile elements display any salient trend with Pt/Pd and Ir/Ru. Empirical and experimental studies suggest that variation of Pt/Pd ratio may result from, apart from sulphide fractionation, (1) fractionation/accumulation of clinopyroxene in which Pt may be moderately compatible (Righter et al., 2004), (2) selective mobilization of Pd or Pt by hydrothermal fluids (Barnes et al., 1985; Wood, 1987; Ballhaus et al., 1994) and (3) fractionation/accumulation of Pt–Ir rich alloys or minerals (Nixon et al., 1993). The former two models cannot satisfactorily explain the Pt/Pd variations in the Taihe western samples because Pt/Pd and PGE abundances in the samples do not vary with MgO (Fig. 5), CaO, and Sc, and the samples are rather fresh and have low LOI.

Highly fractionated Pt/Pd and Ir/Ru are possible, if Pt–Ir rich alloys or minerals have co-precipitated with the sulphides and oxides. The exact cause of alloy or platinum group mineral (PGM) saturation in a magma is debated, but low f_{S2} seems to be favorable (Peck and Keays, 1990; Fleet and Stone, 1991; Tredoux et al., 1995; Maier and Barnes, 1999), as alloys and PGM are found as inclusions in olivine and chromite in ophiolites and layered intrusions (Amosse et al., 1990; Merkle, 1992; Maier and Barnes, 1999; Shi et al., 2007; González-Jiménez et al., 2009, 2012a,b). However, in many oxide- and PGE-mineralized intrusions (e.g. Platinova Reefs, Skaergaard: Andersen et al., 1998; Jinbaoshan, ELIP: Wang et al., 2010), Pt-(Pd)-rich alloys and PGM coexist with sulphides, casting doubt onto the low-f_{S2} explanation. More interestingly, the mafic–ultramafic Tulameen Complex in British Columbia comprises chromitites whose PGE spider patterns are similar to the Taihe western gabbros and Fe–Ti ores, albeit at much higher concentrations, and that the chromitites' positive Pt- and Ir-anomalies have been attributed to the presence of Pt- and Ir-rich alloys (Nixon et al., 1993). That these nuggets in the Tulameen Complex represent magmatic products of early, high temperature crystallization is supported by complete or partial enclosure of euhedral to subhedral cumulus chromite and minor olivine in Pt–Fe alloys (Nixon et al., 1993). Likewise, the high Pt/Pd and Ir/Ru in the western Taihe samples can be rationalized as a result of Pt–Ir rich nugget incorporation, regardless of what determined the precipitation of the nuggets. This model is consistent with our SEM screening where a Pt–Te nugget was identified. The presence of Ir-rich nuggets has not been confirmed by SEM, but this may simply reflect sample bias because only two thin-sections have been scanned but chromite is known to occur within the Taihe gabbros (Shellnutt et al., 2011).

A generalized picture may be that the eastern part of the Taihe gabbro did not undergo sulphide segregation and the PGE variations in the magma were controlled by silicate ± spinel ± Fe–Ti oxide fractionation. In the western part of the pluton, S-saturation seems to be reached and to play an important role in distributing PGEs in the rocks. It appears that the PGE variations are strongly governed by the relative proportion of sulphides + Ir–Pt-rich alloys vs. silicates + oxides accumulated in the rocks. It is convincing that the apparent negative Ru-anomaly of the western Taihe rocks is not a Ru depletion owing to chromite or magnetite fractionation at depth, because the western (negative Ru-anomaly) and eastern (no Ru-anomaly) samples have similar Pd/Ru (25–62 vs. 30–53 respectively). Previous geochemical studies of the Taihe gabbros and associated granitoids favor a relatively closed system for the Taihe Complex (Shellnutt et al., 2011). The currently available PGE data do not dispute this hypothesis, but clearly a better understanding of the stratigraphic relationship of the eastern and western parts of the pluton is needed. This, together with the significant PGE variations within the Taihe gabbroic intrusion as well as the fact that one of the samples has Pt + Pd (>300 ppb) approaching economic grades warrant further studies involving detailed, systematic sampling through the entire stratigraphic section, which was not permitted during the field season of this work.

6.2. Potentials of PGE mineralization in the Panxi region

6.2.1. The overreaching high-Ti and low-Ti distinction of the Emeishan flood basalts

Preceding studies of the Fe–Ti ore-bearing gabbroic and mafic–ultramafic intrusions and their spatially and temporally associated flood basalts and granitoids in the Panxi region have led to the suggestion that these intrusions are genetically related to the high-Ti Emeishan flood basalts, most likely by fractional crystallization (e.g. Pang et al., 2010; Shellnutt and Jahn, 2010;

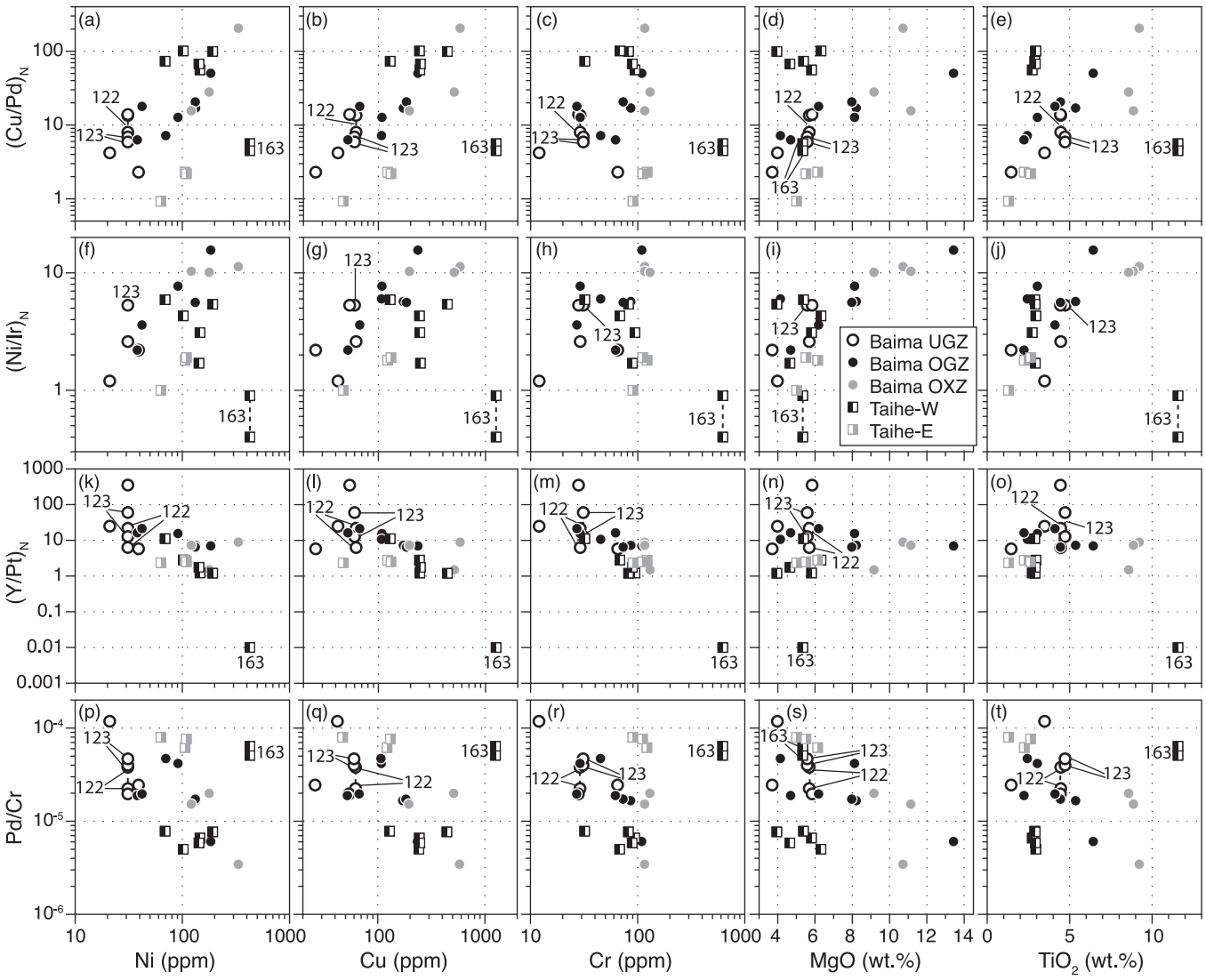

Fig. 8. $(Cu/Pd)_N$, $(Ni/Ir)_N$, $(Y/Pt)_N$ and Pd/Cr vs. Ni, Cu, Cr, MgO and TiO_2 for the Baima and Taihe intrusions. Primitive mantle normalizing values are from Barnes and Maier (1999). UGZ, upper gabbro zone; OGZ, olivine gabbro zone; OXZ, oxide zone. The stratigraphic relationship of UGZ, OGZ and OXZ refers to that of Fig. XX. Duplicate analyses of the same samples are connected by dashed lines.

Shellnutt et al., 2011), although other opinion exists (e.g. Zhong et al., 2011b; Zhou et al., 2013). In contrast, the Ni–Cu-(PGE) sulphide deposits (e.g. Jinbaoshan PGE-rich ultramafic sill; Wang et al., 2010) within the ELIP has been generally thought to be related to the low-Ti magma series. The distinction between the two types of magmas as well as their propensity for certain types of metal (Fe–Ti-[V] vs. Ni–Cu-(PGE)] deposits lead Zhou et al. (2008) to suggest that the two magma series could have been related to the same heterogeneous plume by varying degrees of partial melting: high-Ti series from a Fe-rich, more fertile source accompanied by smaller degrees of partial melting and low-Ti series from a Fe-poor, more refractory source through larger degrees of partial melting. In the model that considers S simply as an incompatible element (e.g. Keays, 1995), the primitive magma of the high-Ti series is more likely S-saturated and that of the low-Ti series more likely S-undersaturated.

Whether the silicate melts are S-saturated or -undersaturated when they leave the mantle source has a strong implication on their PGE contents, as PGEs can be strongly buffered by the retained sulphides in the residual mantle, thereby resulting in PGE-poor melts (Hamlyn et al., 1985; Keays, 1995; Ma et al., 2013a). Whereas this model seems to be self-consistent, the available Emeishan basalt PGE data argue against its simplicity. On plots of ΣPGE vs. Ti/Y and Cu/Pd vs. Ti/Y (Fig. 10a) using the database of Li et al. (2012), the Emeishan basalts and picrites show no correlations among ΣPGE, Cu/Pd and Ti/Y, instead of expected negative trends of ΣPGE–Ti/Y and Cu/Pd–Ti/Y if there was a simple relationship among degrees of partial melting, S-saturation and PGE budgets. The scatter clearly indicates that there is no tendency for high-Ti or low-Ti rocks to be PGE-rich or poor, or S-saturated or -undersaturated. Instead, despite some scatter and with the exception of one low-Ti picrite sample with $\varepsilon Nd_{(T)} = -7.8$, the ΣPGE tends to be lower and Cu/Pd higher at lower $\varepsilon Nd_{(T)}$ (Fig. 10b). This observation is crucial because variation of $\varepsilon Nd_{(T)}$ is generally regarded as evidence of source heterogeneity or crustal contamination in the basaltic system (Shellnutt and Jahn, 2011; Shellnutt, 2014). It is entirely possible that the EFB tapped a heterogeneous source that is varying in terms of its $\varepsilon Nd_{(T)}$ and PGE budget. To account for the scatter in the ΣPGE–Ti/Y and Cu/Pd–Ti/Y plots, this source must also have its individual end-members capable of producing both high-Ti and low-Ti melts. This already argues against the existing model of Zhou et al. (2008) in which the low-Ti magma was initially S-undersaturated and driven to S-saturated through crustal contamination.

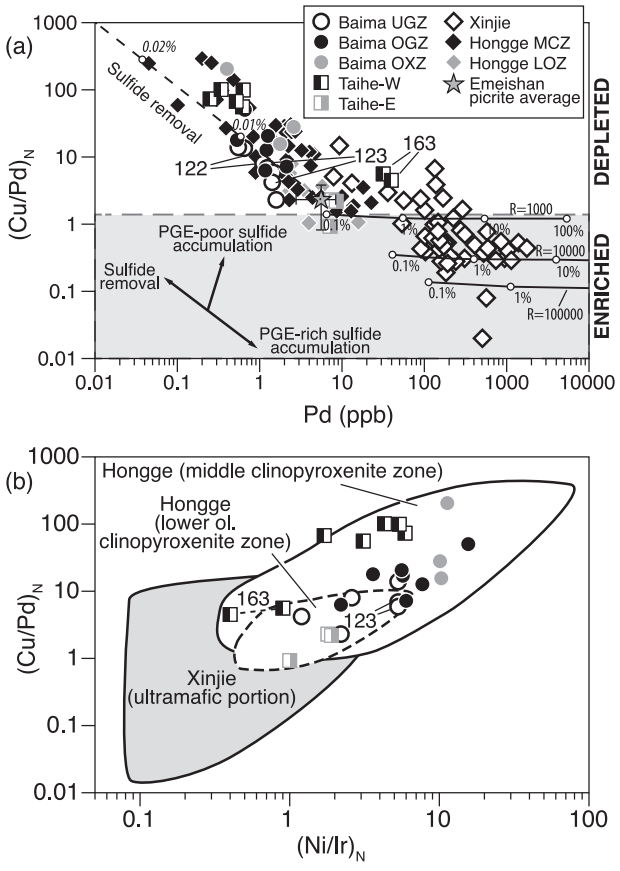

Fig. 9. (a) $(Cu/Pd)_N$ vs. Pd for the Baima and Taihe oxide-bearing gabbroic intrusions, compared with Xinjie intrusions, Hongge intrusions, and the average of Emeishan picrites (Wang et al., 2007; Li et al., 2012) whose standard deviation is shown as bars. Dashed and solid lines show the models of sulphide removal and accumulation, respectively, using the modeling approach of Barnes and Maier (1999). Assuming a magma starting composition as the Emeishan picrite average, a magma undergone sulphide removal would be depleted in Pd and lie along the dashed line. On the other hand, accumulation of a sulphide liquid would produce a cumulate lying along the mixing lines (solid lines) between the silicates and the sulphide liquid. This cumulate is modeled as a three-component mixture, containing (1) a trapped liquid, which is assumed to be 20%, (2) a sulphide liquid, which is the variable in the model (numbers along the solid lines), and (3) a silicate and oxide cumulus phase, which is assumed to have no PGEs. In all the models, the partition coefficients used were $D_{Pd}^{\text{sulphide liq./silicate liq.}} = 25{,}000$ and $D_{Cu}^{\text{sulphide liq./silicate liq.}} = 1000$ (Naldrett, 2010). In each sulphide accumulation model, the metal concentration of the sulphide (C_C) is calculated using the equation of Campbell and Naldrett (1979), $C_C = C_L D(R+1)/(R+D)$, using different R-factors (R), where C_L is the metal concentration of silicate liquid, D is the partition coefficient of the metal between the sulphide and silicate liquids, and R is the mass ratio of silicate to sulphide (i.e. R-factor). The enriched (shaded) and depleted fields are from Barnes and Maier (1999). (b) $(Cu/Pd)_N$ vs. $(Ni/Ir)_N$ for the oxide-bearing intrusions in the Panxi district. In both (a) and (b), data of the Hongge and Xinjie intrusions are from Zhong et al. (2002, 2011a) and Bai et al. (2012). Primitive mantle normalizing values are from Barnes and Maier (1999). Duplicate analyses of the same samples from this study are connected by dashed lines.

Alternatively, S-saturation is controlled largely by crustal contamination regardless of magma series (Keays and Lightfoot, 2010). This appears to be true at least within the ELIP system. The ΣPGE–$\varepsilon Nd_{(T)}$ and Cu/Pd–$\varepsilon Nd_{(T)}$ variations in Fig. 10c and d can be interpreted as source heterogeneity that gives rise to some $\varepsilon Nd_{(T)}$ variation (although there is a lack of PGE data from the picrites with negative $\varepsilon Nd_{(T)}$ values) and on top, crustal contamination that gives rise to additional (lower) $\varepsilon Nd_{(T)}$ variation. The crustal contamination may also drive S-saturation and eventually sulphide segregation, thereby increasing $(Cu/Pd)_N$ while reducing ΣPGE in the magma. To further justify the crustal contamination argument, variations of SiO_2 and trace element ratios such as Th/Nb, which are useful proxies for crustal contamination, against $\varepsilon Nd_{(T)}$ are considered (Fig. 10e and f). In the plots, the EFB data demonstrate their tendency of having higher SiO_2 and Th/Nb at low $\varepsilon Nd_{(T)}$, consistent with the crustal contamination model.

In the following, we compare the Baima and Taihe intrusions with the Xinjie and Hongge intrusions, all of which are thought to be of the high-Ti series, in the context of crustal contamination and prospectivity for PGE mineralization. This comparison is summarized in Table 2. The distinct chalcophile element characteristics of each intrusion as well as the Emeishan basalts are also summarized in a plot of Cu/Pd vs. Ni/Ir on a primitive mantle normalized basis (Fig. 9b), which gives a good proxy for sulphide saturation/segregation.

6.2.2. Xinjie

Among the Panxi Fe–Ti oxide-bearing intrusions, Xinjie is the only one known to contain economic PGE-rich horizons (Table 2; Mao and Sun, 1981; Zhong et al., 2011a). Occurring in the lower part of the intrusion, the PGE-rich horizons have been attributed to the crystallization of Fe–Ti oxides that reduced the oxygen fugacity and depleted Fe in the magma, processes that decreased the sulfur capacity and eventually triggered S-saturation in the Xinjie system (Zhong et al., 2004), although the greater Fe–Ti oxide ores occur in stratigraphically higher up positions than the PGE-rich horizons.

Shown in Fig. 9b, the PGE-rich ores as well as their host ultramafic rocks invariably have high Pd, and low $(Cu/Pd)_N$ and $(Ni/Ir)_N$, implying that the PGE budget in these rocks is controlled by accumulation of a sulphide liquid. Using the approach of Barnes and Maier (1999), the positions of most of these samples on the $(Cu/Pd)_N$–Pd plot can be modeled by assuming them to be a cumulate mixture containing 20% trapped melt, 10% or less sulphides formed at R-factors (ratio of silicate to sulphide liquid; see Campbell and Naldrett, 1979) between 1000 and 10,000, and the rest being silicate and oxide cumulates.

The Xinjie parental magma is clearly more primitive than the Baima and Taihe parental magmas, judging from the intrusion's mafic–ultramafic nature (vs. gabbroic for Baima and Taihe) and from the most-forsteritic olivine of Fo_{88} found in the intrusion (Zhang et al., 2009), an Fo value that would have been equilibrated with a basaltic liquid with Mg# = 69 if $K_D^{ol/liq}$ is 0.3 (Roeder and Emslie, 1970). The fact that the intrusion exhibits low and variable εNd (−5.3 to +2.8) and high $\delta^{18}O$ (up to +8.0) (Zhong et al., 2004; Zhang et al., 2009), and crust-like trace-element signature, such as very high primitive mantle-normalized $(Th/Yb)_N$ (up to 20) (Zhong et al., 2004, 2011a), argues for a significant role of crustal contamination during the evolution of the magma, although available $^{187}Os/^{188}Os$ data from the ultramafic unit remain largely chondritic (Zhong et al., 2011a). The latter may reflect Os isotopes being not a sensitive proxy for crustal contamination (see also Ma et al., 2013b) in this case because of the extremely high Os concentration (up to tens to hundreds of ppb) of the ultramafic rocks compared to the tens-of-ppt levels of continental crust (even lower if the assimilants were carbonates; e.g. Widom et al., 2004). Overall, it can be interpreted that the Xinjie primary magma was initially S-undersaturated and penecontemporaneous with intrusion it became S-saturated as assisted by country rock assimilation which probably provided external S. The segregated sulphides sequestered the PGEs and eventually accumulated as ores.

6.2.3. Hongge

In Hongge, the ultramafic lower part (lower olivine clinopyroxenite zone, LOZ) of the intrusion (Liang et al., 1998) has modest Pd, and $(Cu/Pd)_N$ and $(Ni/Ir)_N$ plotted around unity (Fig. 10). The overlying PGE-depleted pyroxenites and magnetite horizons (middle clinopyroxenite zone, MCZ) have low Pd, and widely variable $(Cu/Pd)_N$ and $(Ni/Ir)_N \geq 1$ (Fig. 9b). These suggest that S-saturated

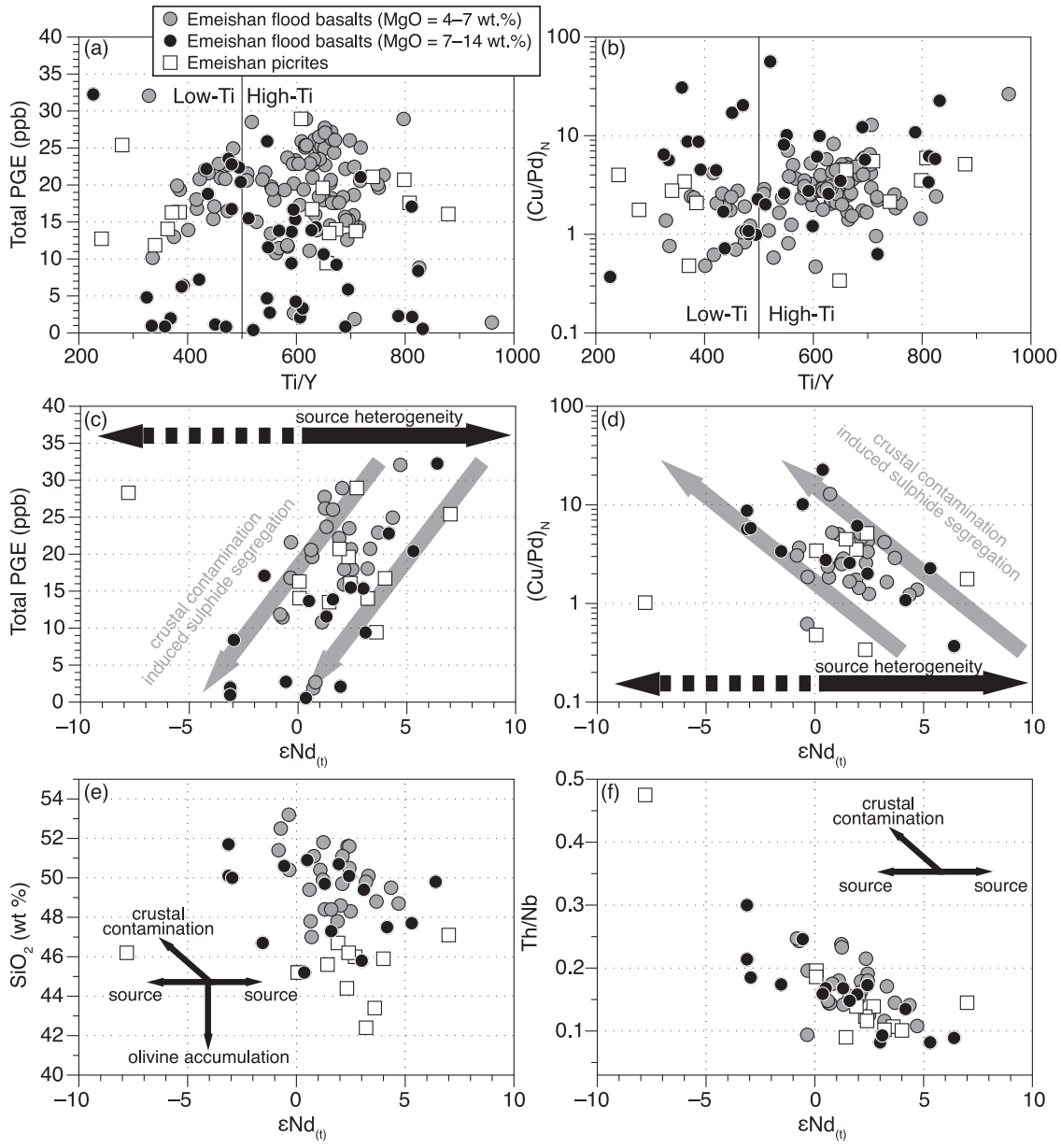

Fig. 10. Total PGE and $(Cu/Pd)_N$ vs. Ti/Y (a, b) and $\varepsilon Nd_{(T)}$ (c and d) and SiO_2 (wt%) and Th/Nb vs. $\varepsilon Nd_{(T)}$ (e, f) for the Emeishan flood basalts and picrites. Data are from Li et al. (2012) and the primitive mantle normalizing values from Barnes and Maier (1999). The division of high-Ti and low-Ti basalts at Ti/Y = 500 is from Xiao et al. (2004).

fractionation occurred in the MCZ and that the saturated sulphides may have been accumulated in this LOZ. Alternatively, the near-unity $(Cu/Pd)_N$ and $(Ni/Ir)_N$ in the LOZ may be interpreted as the primary signature of a magma without prior sulphide segregation. Nevertheless, the positions of the MCZ samples on the $(Cu/Pd)_N$–Pd plot (Fig. 9a) can be modeled by less than 0.02% sulphide segregation.

On the basis of the highest-Fo olivine found in the intrusions (Fo_{88} in Xinjie vs. Fo_{82} in Hongge; data of Zhang et al., 2009), Bai et al. (2012) postulated that the Hongge parental magma is somewhat more evolved and by the time of emplacement the magma had lost a significant portion of PGE through sulphide segregation at depth. Furthermore, the Hongge intrusion carries a less "crust-like" εNd signature than Xinjie ($\varepsilon Nd_{(T)} = -2.7$ to +1.0 in Hongge vs. −5.3 to +2.8 in Xinjie; Zhong et al., 2003, 2004; Zhang et al., 2009), arguing for a less significant role of crustal contamination during the evolution of the Hongge magma. This, together with the more evolved nature of the parental Hongge magma, is considered as the key preventing the intrusion from being PGE mineralized.

6.2.4. Baima

Our PGE data from the Baima intrusion provide a simple picture for the nature of the parental magma and the chalcophile element evolution of this magma. The data exhibit high and somewhat variable $(Cu/Pd)_N$ and $(Ni/Ir)_N$, in conjunction with low and relatively constant PGE concentrations, implying segregation of sulphides at depth or retention in the mantle. Compared to Xinjie and even Hongge, the Baima parental magma is clearly more evolved, with the most magnesian olivine in the intrusion being only ~Fo_{76} (Ma et al., 2003; Shellnutt and Pang, 2012). There is also little crustal signature in the Baima intrusion ($\varepsilon Nd_{(t)} = +1.6$ to +4.2, $(Th/Yb)_N = 0.8$–5.1; Table 2; Shellnutt et al., 2009), implying minimal crustal contamination. All these features suggest that the Baima intrusion is unlikely to contain Cu–Ni and PGE mineralization because using the case of the Xinjie system as

Table 2
Key chalcophile element and chemical features of Fe–Ti oxide-bearing intrusions in the Panxi region, Emeishan Large Igneous Province.

Intrusion	Lithology	Mineralization	$\varepsilon Nd_{(T)}$	Other chemical characteristics	Crustal Cont.	Highest Fo	Par. Mag. S-sat?	Note	$(Cu/Pd)_N$	$(Ni/Ir)_N$	References
Taihe	Mafic	Fe–Ti–V ore	+2.5 to +3.3	$(Th/Yb)_N$ = 1.8–13.2	Minimal	76	Yes		0.9–101	0.4–34 (majority <6)	This study; Shellnutt et al. (2011)
Baima	Mafic	Fe–Ti–V ore	+1.6 to +4.6	$(Th/Yb)_N$ = 0.8–5.1	Minimal	76	No		2.3–205 (majority <50)	1.2–16	This study; Ma et al. (2003); Zhou et al. (2008); Shellnutt et al. (2009); Shellnutt and Pang (2012)
Xinjie	Mafic–ultramafic	Fe–Ti–V ore + Ni–Cu-(PGE) sulphide ore	−5.3 to +2.8	Variable, but generally chondritic $^{187}Os/^{188}Os_{(T)}$; high $\delta^{18}O$ (up to +8.0); high $(Th/Yb)_N$ (4.7–20.7)	Significant	88	No	PGE-rich horizons occur at the base of intrusion, in the ultramafic cumulates and in the gabboric Marginal Unit	<1 in PGE-rich ores and their ultramafic host rocks	<1 in PGE-rich ores and their ultramafic host rocks	Mao and Sun (1981); Zhong et al. (2004, 2011a); Zhang et al. (2009)
Hongge	Mafic–ultramafic	Fe–Ti–V ore	−2.7 to +1.0	$(Th/Yb)_N$ = 0.8–7.5 in MCZ	Significant?	84	Yes?		1.1–7.9 in LOZ; 1.0–291 in MCZ	0.5–5.5 in LCZ; 0.4–66 in MCZ	Liang et al. (1998); Zhong et al. (2002, 2003, 2004); Zhang et al. (2009); Bai et al. (2012)

LOZ: lower olivine clinopyroxene zone; MCZ: middle clinopyroxene zone.

a model, PGE-mineralization requires a combination of all such factors as (1) emplacement of unevolved, S-undersaturated PGE-undepleted magma, immediately followed by or accompanied contemporaneously with (2) effective S-saturation driven by selective S-assimilation through significant crustal contamination at the very early stage of the fractionation crystallization (so that large-scale sulphide segregation may occur almost instantly when some chalcophile elements are still held in the silicate liquid, not in crystal lattices), and (3) perhaps in a very dynamic environment such that the high *R*-factors can promote effective sequestering of the chalcophile elements into the sulphides. None of these factors appears to have been fulfilled in the Baima system.

6.2.5. Taihe

The Taihe system is more complicated, as demonstrated by the fact that the chalcophile element characteristics are systematically different for samples collected from the eastern and western portions of the intrusion. The samples collected from the east are characterized by smooth PGE spidergram patterns and unfractionated $(Cu/Pd)_N$ and $(Ni/Ir)_N$ (Fig. 9b), denoting S-undersaturated fractionation. In contrast, the samples from the west exhibit irregular PGE spidergram patterns, with high Pt/Pd, Ir/Ru, and greater-than-unity $(Cu/Pd)_N$ and $(Ni/Ir)_N$ (Fig. 9b), the latter indicative of sulphide segregation. One exception of this group is an Fe–Ti oxide ore (GS04-163) that shows notably higher PGE concentration (~300 ppb $\sum$PGE) and $(Ni/Ir)_N$ = 0.4 and 0.9 for the two analyses of the same sample, which is the highest concentration of PGEs from ELIP gabbroic intrusions to date, despite its similar PGE spidergram pattern with the other samples of this group. The high PGE concentration and low $(Ni/Ir)_N$ are attributed to alloy and sulphide liquid accumulation.

The parental magma of the Taihe intrusion is thought to be similarly evolved compared to that of the Baima intrusion, because the most-magnesian olivines recorded in both cases are ~Fo_{76} (Shellnutt et al., 2011; Shellnutt and Pang, 2012). Like Baima, the Taihe intrusion also lacks evidence for significant crustal contamination [$\varepsilon Nd_{(t)}$ = +2.5 to + 3.3, $(Th/Yb)_N$ = 1.8–13.2 (majority < 5); Shellnutt et al., 2011]. These features, using our crustal contamination model, would suggest no occurrence of PGE mineralization, which is consistent with the fact that only disseminated sulphides are found at Taihe to date. Although the absence of significant crustal contamination may in theory allow the magma to remain S-undersaturated until a later stage of fractional crystallization, that the sulphides in the Taihe intrusion occur as a disseminated, interstitial phase implies the lack of a critical event to trigger massive segregation of sulphides within a short period of time. It is reasonable to assume that when S-saturation is reached late in the course of fractional crystallization, the sulphides would have low *R*-factors provided that the magmatic system remains largely closed, which is thought to be the case of Taihe (Shellnutt et al., 2011). Using the oxide ore sample GS04-163 as an example of relatively PGE-rich, sulphide-bearing rocks in Taihe, its position on the $(Cu/Pd)_N$–Pd plot suggests an *R*-factor lower than 1000, 1–2 orders of magnitude lower than that modeled for the majority of Xinjie samples.

7. Conclusions

The platinum group elemental data from the Baima gabbroic rocks is consistent with a fractionation model of a relatively evolved, mafic, S-undersaturated parental magma. The data presented here indicate that the Baima intrusion was affected by sulphide segregation and that the probability of economic concentrations of PGEs is low. In contrast, Taihe gabbroic rocks reveal a systematically different system despite the likelihood of a similar parental magma. The Taihe gabbros show evidence for both

S-saturated and S-undersaturated samples and that the parental magma was likely emplaced very close to S-saturation. The lack of substantial crustal contamination may have allowed the magma to remain S-undersaturated for a longer duration of magma crystallization. Although PGE and sulphide mineralization has not been found in the Taihe intrusion, the presence of one sub-economic PGE-enriched sample (Pt + Pd ≈300 ppb) suggests that the parental magma likely did not experience sulphide segregation and is an encouraging site for further prospecting.

Acknowledgements

We would like to thank Prof. Mei-Fu Zhou for his comments on an earlier draft of this manuscript, K. Heide for editorial handling and two anonymous reviewers for their constructive comments. JGS thanks the National Science Council of Taiwan for their support through grant NSC102-2628-M-003-001-MY4. GSKM is supported by an Academia Sinica Postdoctoral Fellowship.

References

Ali, J.R., Thompson, G.M., Zhou, M.-F., Song, X.Y., 2005. Emeishan large igneous province, SW China. Lithos 79, 475–489.

Amosse, J., Allibert, M., Fischer, W., Piboule, M., 1990. Experimental study of the solubility of platinum and iridium in basic silicate melts–implications for the differentiation of platinum-group elements during magmatic processes. Chem. Geol. 81, 45–53.

Andersen, J.C.O., Rasmussen, H., Nielsen, T.F.D., Ronsbo, J.G., 1998. The Triple Group and the Platinova gold and palladium reefs in the Skaergaard Intrusion; stratigraphic and petrographic relations. Econ. Geol. 93, 488–509.

Andersen, J.C.Ø., 2006. Postmagmatic sulphur loss in the Skaergaard Intrusion: implications for the formation of the Platinova Reef. Lithos 92, 198–221.

Bai, Z.-J., Zhong, H., Li, C., Zhu, W.-G., Xu, G.-W., 2012. Platinum-group elements in the oxide layers of the Hongge mafic–ultramafic intrusion, Emeishan Large Igneous Province, SW China. Ore Geol. Rev. 46, 149–161.

Ballhaus, C., Ryan, C.G., Mernagh, T.P., Green, D.H., 1994. The partitioning of Fe, Ni, Cu, Pt, and Au between sulphide, metal, and fluid phases. A pilot study. Geochim. Cosmochim. Acta 58, 811–826.

Barnes, S.-J., Maier, W.D., 1999. The fractionation of Ni, Cu and the noble metals in silicate and sulphide liquids. In: Keays, R.R., Lesher, C.M., Lightfoot, P.C., Farrow, C.E.G. (Eds.), Dynamic Processes in Magmatic Ore Deposits and Their Application in Mineral Exploration, Short Course Volume 13. Geological Association of Canada, pp. 69–106.

Barnes, S.-J., Naldrett, A.J., Gorton, M.P., 1985. The origin of the fractionation of platinum-group elements in terrestrial magmas. Chem. Geol. 53, 303–323.

Brenan, J.M., Finnigan, C.F., McDonough, W.F., Homolova, V., 2012. Experimental constraints on the partitioning of Ru, Rh, Ir, Pt and Pd between chromite and silicate melt: the importance of ferric iron. Chem. Geol. 302–303, 16–32.

Brügmann, G.E., Naldrett, A.J., Asif, M., Lightfoot, P.C., Gorbachev, N.S., Fedorenko, V.A., 1993. Siderophile and chalcophile metals as tracers of the evolution of the Siberian Trap in the Noril'sk region, Russia. Geochim. Cosmochim. Acta 57, 2001–20018.

Buchl, A., Brugmann, G., Batanova, V.G., 2004. Formation of podiform chromatite deposits: implications from PGE abundances and Os isotopic compositions of chromites from the Troodos complex, Cyprus. Chem. Geol. 208, 217–232.

Campbell, I.H., Naldrett, A.J., 1979. The influence of sulphide:silicate ratios on the geochemistry of magmatic sulphides. Econ. Geol. 74, 1503–2150.

Chen, F., 1990. Petrologic study on Baima ore-bearing layered mafic–ultramafic intrusion. Acta Petr. Sin. 4, 13–26 (in Chinese with English abstract).

Chung, S.-L., Jahn, B.-M., 1995. Plume-lithosphere interaction in generation of the Emeishan flood basalts at the Permian-Triassic boundary. Geology 23, 889–892.

Crocket, J.H., Paul, D.K., 2004. Platinum-group elements in Deccan mafic rocks: a comparison of suites differentiated by Ir content. Chem. Geol. 208, 273–291.

Fan, W., Zhang, C., Wang, Y., Guo, F., Peng, T., 2008. Geochronology and geochemistry of Permian basalts in western Guangxi Province, southwest China: evidence for plume-lithosphere interaction. Lithos 102, 218–236.

Fleet, M.E., Stone, W.E., 1991. Partitioning of platinum-group elements in the Fe-Ni-S system and their fractionation in nature. Geochim. Cosmochim. Acta 55, 245–253.

Ganino, C., Arndt, N.T., Zhou, M.-F., Gaillard, F., Chauvel, C., 2008. Interaction of magma with sedimentary wall rock and magnetite ore genesis in the Panzhihua mafic intrusion, SW China. Miner. Deposita 43, 677–694.

González-Jiménez, J.M., Gervilla, F., Griffin, W.L., Proenza, J.A., Augé, T., O'Reilly, S.Y., Pearson, N.J., 2012a. Os-isotope variability within sulphides from podiform chromitites. Chem. Geol. 291, 224–235.

González-Jiménez, J.M., Gervilla, F., Proenza, J.A., Kerestedjian, T., Augé, T., Bailly, L., 2009. Zoning of laurite (RuS_2)-erlichmanite (OsS_2): implications for the origin of PGM in ophiolite chromitites. Eur. J. Miner. 21, 419–432.

González-Jiménez, J.M., Griffin, W.L., Gervilla, F., Kerestedjian, T.N., O'Reilly, S.Y., Proenza, J.A., Pearson, N.J., Sergeeva, I., 2012b. Metamorphism disturbs the Re-Os signatures of platinum-group minerals in ophiolite chromitites. Geology 40, 659–662.

Hamlyn, P.R., Keays, R.R., Cameron, W.E., Crawford, A.J., Waldron, H.M., 1985. Precious metals in magnesian low-Ti lavas: implications for metallogenesis and sulfur saturation in primary magmas. Geochim. Cosmochim. Acta 49, 1797–1811.

He, B., Xu, Y.-G., Huang, X.-L., Luo, Z.-Y., Shi, Y.-R., Yang, O.-J., Yu, S.-Y., 2007. Age and duration of the Emeishan flood volcanism, SW China: Geochemistry and SHRIMP zircon U–Pb dating of silicic ignimbrites, post-volcanic Xuanwei Formation and clay tuff at the Chaotian section. Earth Planet. Sci. Lett. 255, 306–323.

Hou, T., Zhang, Z., Encarnacion, J., Santosh, M., 2012. Petrogenesis and metallogenesis of the Taihe gabbroic intrusion associated with Fe-Ti-oxide ores in the Panxi district, Emeishan large igneous province southwest, China. Ore Geol. Rev., http://dx.doi.org/10.1016/j.oregeorev.2012.09.004.

Keays, R.R., 1995. The role of komatiitic and picritic magmatism and S-saturation in the formation of ore deposits. Lithos 34, 1–18.

Keays, R.R., Lightfoot, P.C., 2010. Crustal sulfur is required to form magmatic Ni–Cu sulphide deposits: evidence from chalcophile element signatures of Siberian and Deccan Trap basalts. Miner. Deposita 45, 241–257.

Li, C., Tao, Y., Qi, L., Ripley, E.M., 2012. Controls on PGE fractionation in the Emeishan picrites and basalts: constraints from integrated lithophile–siderophile elements and Sr–Nd isotopes. Geochim. Cosmochim. Acta 90, 12–32.

Liang, Y.B., Liu, T.Y., Song, G.R., Jin, Z.M., 1998. Platinum Group Element Deposits in China. Metallurgical Industry Press, Beijing (in Chinese).

Lightfoot, P.C., Keays, R.R., 2005. Siderophile and chalcophile metal variations in flood basalts 546 from the Siberian trap, Noril'sk region: implications for the origin of the Ni-Cu-PGE 547 sulphide ores. Econ. Geol. 100, 439–462.

Liu, D., Jian, P., Kröner, A., Xu, S., 2006. Dating of prograde metamorphic events deciphered from episodic zircon growth in rocks of the Dabie–Sulu UHP complex, China. Earth Planet. Sci. Lett. 250, 650–666.

Ma, G.S.-K., Malpas, J., Gao, J.F., Wang, K.-L., Qi, L., Xenophontos, C., 2013a. Platinum-group element geochemistry of intraplate basalts from the Aleppo Plateau, NW Syria. Geol. Mag. 150, 497–508.

Ma, G.S.-K., Malpas, J., Suzuki, K., Lo, C.H., Wang, K.L., Iizuka, Y., Xenophontos, C., 2013b. Evolution and origin of the Miocene intraplate basalts on the Aleppo Plateau. NW Syria. Chem. Geol. 335, 149–171.

Ma, Y., Ji, X.T., Li, J.C., Huang, M., Kan, Z.Z., 2003. Mineral Resources of the Panzhihua Region. Sichuan Science and Technology Press, Chengdu, pp. 275 (in Chinese).

Maier, W.D., Barnes, S.J., 1999. Platinum-group elements in silicate rocks of the Lower, Critical and Main Zones at union section, western Bushveld Complex. J. Petrol. 40, 1647–1671.

Maier, W.D., Barnes, S.-J., Gartz, V., Andrews, G., 2003. Pt–Pd reefs in magnetitites of the Stella layered intrusion, South Africa: a world of new exploration opportunities for platinum group elements. Geology 31, 885–888.

Mao, Y., Sun, S., 1981. Petrological characteristics and origin of layered basic-ultrabasic intrusions in Xinjie Miyi Sichuan. J. Mineral. Petrol. 6, 29–40.

Mavrogenes, J.A., O'Neill, H.S.C., 1999. The relative effects of pressure, temperature and oxygen fugacity on the solubility of sulphide in mafic magmas. Geochim. Cosmochim. Acta 63, 1173–1180.

McDonough, W.F., Sun, S.-S., 1995. The composition of the Earth. Chem. Geol. 120, 223–253.

Merkle, R.K.W., 1992. Platinum-group minerals in the middle group of chromitite layers at Marikana, western Bushveld Complex: indications for collection mechanisms and postmagmatic modification. Can. J. Earth Sci. 29, 209–221.

Mungall, J.E., Hanley, J.J., Arndt, N.T., Debecdelievre, A., 2006. Evidence from meimechites and other low-degree mantle melts for redox controls on mantle-crust fractionation of platinum-group elements. Proc. Natl. Acad. Sci. 103, 12695–12700.

Naldrett, A.J., 2010. Secular variation of magmatic sulphide deposits and their source magmas. Econ. Geol. 105, 669–688.

Naldrett, A.J., Wilson, A., Kinnaird, J., Yudovskaya, M., Chunnett, G., 2012. The origin of chromitites and related PGE mineralization in the Bushveld Complex: new mineralogical and petrological constraints. Miner. Deposita, http://dx.doi.org/10.1007/s00126-011-0366-3.

Nixon, G.T., Hammack, J.L., Ash, C.A., Cabri, L.J., Case, G., Connelly, J.N., Heaman, L.M., Laflamme, J.H.G., Nuttall, C., Paterson, W.P.E., Wong, R.H., 1993. Platinum-Group-Element Mineralization. Geology and Platinum-Group-Element Mineralization of Alaskan-Type Ultramafic-Mafic Complexes in British Columbia. British Columbia Geological Survey, Bulletin 93: Ministry of Employment and Investment, pp. 87–118.

O'Neill, H.St.C., Mavrogenes, J.A., 2002. The sulphide capacity and the sulfur content at sulphide saturation of silicate melts at 1400 °C and 1 bar. J. Petrol. 43, 1049–1087.

Pagé, P., Barnes, S.-J., Bédard, J.H., Zientek, M.L., 2012. In situ determination of Os, Ir, and Ru in chromites formed from komatiite, tholeiite and boninite magmas: implications for chromite control of Os, Ir and Ru during partial melting and crystal fractionation. Chem. Geol. 302–303, 3–15.

Palme, H., O'Neill, H.S.C., 2003. Cosmochemical estimates of mantle composition. In: Carlson, R.W. (Ed.), The Mantle and Core. Treatise on Geochemistry 2. Elsevier-Pergamon, Oxford, pp. 1–38.

Pang, K.-N., Zhou, M.-F., Qi, L., Shellnutt, J.G., Wang, C.Y., Zhao, D., 2010. Magmatic Fe–Ti–V oxide deposits in the Emeishan large igneous province, SW China. Lithos 119, 123–136.

Park, J.-W., Hu, Z., Gao, S., Campbell, I.H., Gong, H., 2012a. Platinum group element abundances in the upper continental crust revisited – new constraints from analyses of Chinese loess. Geochim. Cosmochim. Acta 93, 63–76.

Park, J.-W., Campbell, I.H., Eggins, S.M., 2012b. Enrichment of Rh, Ru, Ir and Os in Cr spinels from oxidized magmas: evidence from the Ambae volcano, Vanuatu. Geochim. Cosmochim. Acta 78, 28–50.
Peach, C.L., Mathez, E.A., Keays, R.R., Reeves, S.J., 1994. Experimentally-determined sulphide melt–silicate melt partition coefficients for iridium and palladium. Chem. Geol. 117, 361–377.
Peck, D.C., Keays, R.R., 1990. Insights into the behavior of precious metals in primitive, S-undersaturated magmas; evidence from the Heazlewood River complex, Tasmania. Can. Min. 28, 553–577.
Puchtel, I.S., Humayun, M., 2001. Platinum group element fractionation in a komatiitic basalt lava lake. Geochim. Cosmochim. Acta 65, 2979–2993.
Qi, L., Zhou, M.-F., 2008. Determination of platinum-group elements in OPY-1: comparison of results using different digestion techniques. Geost. Geoanal. Res. 32, 377–387.
Qi, L., Zhou, M.-F., Wang, C.Y., 2004. Determination of low concentrations of platinum group elements in geological samples by ID-ICP-MS. J. Anal. Atom. Spectrom. 19, 1335–1339.
Qi, L., Zhou, M.-F., Wang, C.Y., Sun, M., 2007. Evaluation of a technique for determining Re and PGEs in geological samples by ICP-MS coupled with a modified Carius tube digestion. Geochem. J. 41, 407–414.
Righter, K., Campbell, A.J., Humayun, M., Hervig, R.L., 2004. Partitioning of Ru, Rh, Pd, Re, Ir, and Au between Cr-bearing spinel, olivine, pyroxene and silicate melts. Geochim. Cosmochim. Acta 68, 867–880.
Roeder, P.L., Emslie, R.F., 1970. Olivine-liquid equilibrium. Contrib. Mineral. Petr. 29, 275–289.
Shellnutt, J.G., 2014. The Emeishan large igneous province: a synthesis. Geosci. Front. 5, 369–394.
Shellnutt, J.G., Pang, K.-N., 2012. Mineral compositions of the Late Permian Baima layered gabbroic intrusion: constraints on petrogenesis. Mineral. Petrol. 106, 75–88.
Shellnutt, J.G., Denyszyn, S., Mundil, R., 2012. Precise age determination of mafic and felsic intrusive rocks from the Permian Emeishan large igneous province (SW China). Gondwana Res. 22, 118–126.
Shellnutt, J.G., Wang, K.-L., Zellmer, G.F., Iizuka, Y., Jahn, B.-M., Pang, K.-N., Qi, L., Zhou, M.-F., 2011. Three Fe-Ti oxide ore-bearing gabbro-granitoid complexes in the Panxi region of the Emeishan large igneous province, SW China. Am. J. Sci. 311, 773–812.
Shellnutt, J.G., Wang, K.-L., 2014. An ultramafic primary magma for a low Si, high Ti-Fe gabbro in the Panxi region of the Emeishan large igneous province, SW China. J. Asian Earth Sci. 79, 329–344.
Shellnutt, J.G., Jahn, B.-M., 2011. Origin of Late Permian Emeishan basaltic rocks from the Panxi region (SW China): implications for the Ti-classification and spatial-compositional distribution of the Emeishan basalts. J. Volcanol. Geoth. Res. 199, 85–95.
Shellnutt, J.G., Jahn, B.-M., Dostal, J., 2010. Elemental and Sr-Nd isotope geochemistry of microgranular enclaves from peralkaline A-type granitic plutons of the Emeishan large igneous province, SW China. Lithos 119, 34–46.
Shellnutt, J.G., Jahn, B.-M., 2010. Formation of the Late Permian Panzhihua plutonic-hypabyssal-volcanic igneous complex: implications for the genesis of Fe-Ti oxide deposits and A-type granites of SW China. Earth Planet. Sci. Lett. 289, 509–519.
Shellnutt, J.G., Zhou, M.-F., Zellmer, G., 2009. The role of Fe–Ti oxide crystallization in the formation of A-type granitoids with implications for the Daly gap: an example from the Permian Baima igneous complex, SW China. Chem. Geol. 259, 204–217.
Shellnutt, J.G., Zhou, M.-F., Yan, D.-P., Wang, Y., 2008. Longevity of the Permian Emeishan mantle plume (SW China): 1 million years; 8 million years or 18 million years? Geol. Mag. 145, 373–388.
Shellnutt, J.G., Zhou, M.-F., 2007. Permian peralkaline, peraluminous and metaluminous A-type granites in the Panxi district, SW China: their relationship to the Emeishan mantle plume. Chem. Geol. 243, 286–316.
Shi, R., Alard, O., Zhi, X., O'Reilly, S.Y., Pearson, N.J., Griffin, W.L., Zhang, M., Chen, X., 2007. Multiple events in the Neo-Tethyan oceanic upper mantle: evidence from Ru–Os–Ir alloys in the Luobusa and Dongqiao ophiolitic podiform chromitites, Tibet. Earth Planet. Sci. Lett. 261, 33–48.
Song, X.-Y., Zhou, M.-F., Cao, Z.-M., Sun, M., Wang, Y.-L., 2003. Ni-Cu-(PGE) magmatic sulphide deposits in the Yangliuping area, Permian Emeishan igneous province, SW China. Miner. Deposita 38, 831–843.
Song, X.-Y., Zhou, M.-F., Keays, R.R., Cao, Z.-M., Sun, M., Qi, L., 2008. Geochemistry of the Emeishan flood basalts at Yangliuping, Sichuan, SW China: implications for sulphide segregation. Contrib. Mineral. Petr. 152, 53–74.
Tao, Y., Li, C., Hu, R., Qi, L., Qu, W., Du, A., 2010. Re-Os isotopic constraints on the genesis of the Limahe Ni–Cu deposit in the Emeishan large igneous province, SW China. Lithos 119, 137–146.
Tredoux, M., Kindsay, N.M., Davies, G., McDonald, I., 1995. The fractionation of platinum-group elements in magmatic systems, with the suggestion of a novel causal mechanism. S. Afr. J. Geol. 98, 157–167.
Vogel, D.C., Keays, R.R., 1997. The petrogenesis and platinum-group element geochemistry of the Newer Volcanic Province, Victoria, Australia. Chem. Geol. 136, 181–204.
Wang, D.R., Xie, Y.M., Hu, Y.J., You, X.X., Cao, J.X., 1993. Geology of Guogailiang area (Map G-48-1-A). Panxi Geological Team, Geology and Mineral Resources Bureau, Sichuan Province, 1: 50000.
Wang, D.R., Xie, Y.M., Wang, Q.J., Tao, Z.D., 1994. Geology of Guabang area (Map G-48-25-C). Panxi Geological Team, Geology and Mineral Resources Bureau, Sichuan Province, 1: 50000.
Wang, C.Y., Zhou, M.-F., Keays, R.R., 2006. Geochemical constraints on the origin of the Permian Baimazhai mafic–ultramafic intrusion, SW China. Contrib. Mineral. Petr. 152, 309–321.
Wang, C.Y., Zhou, M.-F., Qi, L., 2007. Permian flood basalts and mafic intrusions in the Jinping (SW China)–Song Da (northern Vietnam) district: Mantle sources, crustal contamination and sulphide segregation. Chem. Geol. 243, 317–343.
Wang, C.Y., Zhou, M.-F., Qi, L., 2010. Origin of extremely PGE-rich mafic magma system: an example from the Jinbaoshan ultramafic sill, Emeishan large igneous province, SW China. Lithos 119, 147–161.
Widom, E., Gaddis, S.J., Wells Jr., N.E., 2004. Re-Os isotope systematics in carbonates from Serpent Mound, Ohio: Implications for Re-Os dating of crustal rocks and the osmium isotopic composition of Ordovician seawater. Geochem. Geophys. Geosyst. 5, http://dx.doi.org/10.1029/2002gc000444.
Wood, S.A., 1987. Thermodynamic calculations of the volatility of the platinum group elements (PGE): the PGE content of fluids at magmatic temperatures. Geochim. Cosmochim. Acta 51, 3041–3050.
Xiao, L., Xu, Y.G., Mei, H.J., Zheng, Y.F., He, B., Pirajno, F., 2004. Distinct mantle sources of low-Ti and high-Ti basalts from the western Emeishan large igneous province, SW China: implications for plume–lithosphere interaction. Earth Planet. Sci. Lett. 228, 525–546.
Xu, Y.-G., Luo, Z.-Y., Huang, X.-L., He, B., Xiao Xie, L.-W., Shi, Y.-R., 2008. Zircon U–Pb and Hf isotope constraints on crustal melting associated with the Emeishan mantle plume. Geochim. Cosmochim. Acta 72, 3084–3104.
Xu, Y.-G., He, B., Chung, S.L., Menzies, M., Frey, F.A., 2004. Geologic, geochemical, and geophysical consequences of plume involvement in the Emeishan flood-basalt province. Geology 32, 917–920.
Xu, Y.-G., Chung, S.L., Jahn, B-M., Wu, G., 2001. Petrologic and geochemical constraints on the petrogenesis of Permian-Triassic Emeishan flood basalts in southwestern China. Lithos 58, 145–168.
Yang, R., Xu, W., Liu, R., 1997. REE geochemistry of Baima complex in the Panxi rift belt. Acta Mineral. Sin. 17, 71–77 (in Chinese).
Zhang, Z., Mao, J., Saunders, A.D., Ai, Y., Li, Y., Zhao, L., 2009. Petrogenetic modeling of three mafic-ultramafic layered intrusions in the Emeishan large igneous province, SW China, based on isotopic and bulk chemical constraints. Lithos 113, 369–392.
Zhong, H., Qi, L., Hu, R.-Z., Zhou, M.-F., Gou, T.-Z., Zhu, W.-G., Liu, B.-G., Chu, Z.-Y., 2011a. Rhenium–osmium isotope and platinum-group elements in the Xinjie layered intrusion, SW China: Implications for source mantle composition, mantle evolution, PGE fractionation and mineralization. Geochim. Cosmochim. Acta 75, 1621–1641.
Zhong, H., Qi, L., Hu, R.-Z., Zhou, M.-F., Gou, T.-Z., Zhu, W.-G., Liu, B.-G., Chu, Z.-Y., 2011b. Timing and source constraints on the relationship between mafic and felsic intrusions in the Emeishan large igneous province. Geochim. Cosmochim. Acta 75, 1374–1395.
Zhong, H., Yao, Y., Hu, S.F., Zhou, X.H., Liu, B.G., Sun, M., Zhou, M.-F., Viljoen, M.J., 2003. Trace-element and Sr-Nd isotopic geochemistry of the PGE-bearing Hongge layered intrusion, southwestern China. Int. Geol. Rev. 45, 371–382.
Zhong, H., Yao, Y., Prevec, S.A., Wilson, A.H., Viljoen, M.J., Viljoen, R.P., Liu, B.-G., Luo, Y.-N., 2004. Trace-element and Sr–Nd isotopic geochemistry of the PGE-bearing Xinjie layered intrusion in SW China. Chem. Geol. 203, 237–252.
Zhong, H., Zhou, X.H., Zhou, M.-F., Sun, M., Liu, B.G., 2002. Platinum-group element geochemistry of the Hongge Fe-V-Ti deposit in the Pan-Xi area, southwestern China. Miner. Deposita 37, 226–239.
Zhou, M.-F., Sun, M., Keays, R.R., Kerrich, R., 1998. Controls on the platinum-group elemental distributions in high-Cr and high-Al chromitites: a case study of the podiform chromitites from the Chinese orogenic belts. Geochim. Cosmochim. Acta 62, 677–688.
Zhou, M.-F., Robinson, P.T., Lesher, C.M., Keays, R.R., Zhang, C.J., Malpas, J., 2005. Geochemistry, petrogenesis and metallogenesis of the Panzhihua gabbroic layered intrusion and associated Fe–Ti–V oxide deposits, Sichuan Province, SW China. J. Petrol. 46, 2253–2280.
Zhou, M.-F., Arndt, N.T., Malpas, J., Wang, C.Y., Kennedy, A.K., 2008. Two magma series and associated ore deposit types in the Permian Emeishan large igneous province, SW China. Lithos 103, 352–368.
Zhou, M.-F., Chen, W.T., Wang, C.Y., Prevec, S.A., Liu, P.P., Howarth, G.H., 2013. Two stages of immiscible liquid separation in the formation of Panzhihua-type Fe–Ti–V oxide deposits, SW China. Geosci. Front., http://dx.doi.org/10.1016/j.gf.f.2013.04.006.